

# JGR Atmospheres

## RESEARCH ARTICLE

10.1029/2019JD031159

This article is a companion to Mardi et al. (2018) <https://doi.org/10.1029/2018JD029134>.

### Key Points:

- Primary activation of sub-cloud CCN was the key driver of cloud droplet concentration ( $N_d$ ) in biomass burning (BB) and non-BB conditions
- Relationships between  $N_d$  and either droplet effective radius ( $r_e$ ) or rain rate (R) are similar regardless of the level of BB influence
- Cloud water and droplet residual particle composition differed between BB and non-BB conditions

### Supporting Information:

- Supporting Information S1

### Correspondence to:

A. Sorooshian,  
[armin@email.arizona.edu](mailto:armin@email.arizona.edu)

### Citation:

Mardi, A. H., Dadashazar, H., MacDonald, A. B., Crosbie, E., Coggon, M. M., Aghdam, M. A., et al. (2019). Effects of biomass burning on stratocumulus droplet characteristics, drizzle rate, and composition. *Journal of Geophysical Research: Atmospheres*, 124, 12,301–12,318. <https://doi.org/10.1029/2019JD031159>











Received 12 JUN 2019

Accepted 29 OCT 2019

Accepted article online 7 NOV 2019

Published online 28 NOV 2019

## Effects of Biomass Burning on Stratocumulus Droplet Characteristics, Drizzle Rate, and Composition

Ali Hossein Mardi<sup>1</sup> , Hossein Dadashazar<sup>1</sup> , Alexander B. MacDonald<sup>1</sup> , Ewan Crosbie<sup>2,3</sup> , Matthew M. Coggon<sup>4</sup> , Mojtaba Azadi Aghdam<sup>1</sup> , Roy K. Woods<sup>5</sup> , Hafliði H. Jonsson<sup>5</sup>, Richard C. Flagan<sup>6</sup> , John H. Seinfeld<sup>6</sup> , and Armin Sorooshian<sup>1,7</sup> 

<sup>1</sup>Department of Chemical and Environmental Engineering, University of Arizona, Tucson, AZ, USA, <sup>2</sup>Science Systems and Applications, Inc., Hampton, VA, USA, <sup>3</sup>NASA Langley Research Center, Hampton, VA, USA, <sup>4</sup>Cooperative Institute for Research in Environmental Science and National Oceanic and Atmospheric Administration, Boulder, CO, USA, <sup>5</sup>Naval Postgraduate School, Monterey, CA, USA, <sup>6</sup>Department of Chemical Engineering, California Institute of Technology, Pasadena, CA, USA, <sup>7</sup>Department of Hydrology and Atmospheric Sciences, University of Arizona, Tucson, AZ, USA

**Abstract** This study reports on airborne measurements of stratocumulus cloud properties under varying degrees of influence from biomass burning (BB) plumes off the California coast. Data are reported from five total airborne campaigns based in Marina, California, with two of them including influence from wildfires in different areas along the coast of the western United States. The results indicate that subcloud cloud condensation nuclei number concentration and mass concentrations of important aerosol species (organics, sulfate, nitrate) were better correlated with cloud droplet number concentration ( $N_d$ ) as compared to respective above-cloud aerosol data. Given that the majority of BB particles resided above cloud tops, this is an important consideration for future work in the region as the data indicate that the subcloud BB particles likely were entrained from the free troposphere. Lower cloud condensation nuclei activation fractions were observed for BB-impacted clouds as compared to non-BB clouds due, at least partly, to less hygroscopic aerosols. Relationships between  $N_d$  and either droplet effective radius or drizzle rate are preserved regardless of BB influence, indicative of how parameterizations can exhibit consistent skill for varying degrees of BB influence as long as  $N_d$  is known. Lastly, the composition of both droplet residual particles and cloud water changed significantly when clouds were impacted by BB plumes, with differences observed for different fire sources stemming largely from effects of plume aging time and dust influence.

## 1. Introduction

An extensively studied cloud type influenced greatly by aerosols is stratocumulus (Sc). This is the dominant cloud type by area globally (Warren et al., 1986), covering approximately one fifth of the Earth surface on an annual basis (Wood, 2012). These clouds are climatically very important as their shortwave cloud albedo forcing is larger than their longwave cloud greenhouse forcing, resulting in net cooling over the regions they cover (Chen et al., 2000; Harrison et al., 1990; Hartmann & Short, 1980; Herman et al., 1980; Stephens & Greenwald, 1991). The role of these clouds in Earth's radiation budget is significant as a small variation in their microphysical properties can lead to a large impact on Earth's energy balance. For instance, Slingo (1990) reported that the radiative impact exerted by doubling of carbon dioxide ( $\text{CO}_2$ ) can be offset under the following circumstances: (i) 15–20% increase in amount of low clouds, (ii) 20–35% increase in liquid water path (LWP), and (iii) 15–20% decrease in mean droplet effective radius ( $r_e$ ). In another study, Jones et al. (2009) suggested that a modification of Sc microphysical properties via geoengineering activities can partially offset radiative forcing associated with greenhouse gas levels.

The northeast Pacific (NEP) Ocean region is home to one of the three major Sc decks in the world and is impacted by multiple wildfire incidents annually, with the prevalence and severity of events expected to increase in coming years (Barbero et al., 2015; Dennison et al., 2014; Flannigan et al., 2000; Hallar et al., 2017; Moritz et al., 2012). The general transport pattern of plumes from fires near the western United States coast results in biomass burning (BB) particles both above and within the marine boundary layer (MBL; Mardi et al., 2018). This motivates BB-Sc interaction studies owing to the impact BB plumes can have on the MBL (Brioude et al., 2009; Johnson et al., 2004), with poorly characterized and potentially different effects if the plumes reside either above or below the cloud deck.

There is a growing number of field studies investigating the role of BB particles in both serving as cloud condensation nuclei (CCN) and altering cloud microphysical properties. Recent examples in the southeast Atlantic (SEA) region were reviewed by Zuidema et al. (2016) and include ObseRvations of Aerosols above CLouds and their intEractionS, Layered Atlantic Smoke Interactions with Clouds, Aerosol Radiation and Clouds in southern Africa, and Clouds and Aerosol Radiative Impacts and Forcing: Year 2016, in addition to older campaigns such as the Southern African Regional Science Initiative (SAFARI 2000; Swap et al., 2002). Past work has examined the vertical distribution of BB aerosols relative to the Sc deck and the extent to which BB layers in the SEA region remain well separated from the underlying Sc deck (Das et al., 2017; Lu et al., 2018; Rajapakshe et al., 2017). The vertical distance between BB aerosols and the Sc deck plays a vital role in BB layer impact on Sc radiative properties (Costantino & Bréon, 2010, 2013; Diamond et al., 2018; Koch & Del Genio, 2010; Wilcox, 2012).

While there has been extensive research focused on the SEA region for BB-Sc interactions, less is known about BB-Sc interactions over the NEP region, which traditionally has received attention due to extensive shipping that leads to strong aerosol perturbations that facilitate aerosol-cloud interaction research (e.g., Russell et al., 2013; Sorooshian et al., 2019). Wildfires over the western United States, especially along the coast (Dadashazar et al., 2019; Maudlin et al., 2015; Schlosser et al., 2017), allow for an opportunity to examine how strongly aerosol perturbations in a form other than shipping impacts the Sc deck. The current study serves as the second part to a previous study (Mardi et al., 2018), which investigated characteristics of the BB plumes (e.g., altitude, location relative to cloud top height, thickness, number of vertically adjacent layers, interlayer distances, and aerosol size distributions) and vertical profiles of shortwave heating rates in the presence of BB plumes. This study uses the same data set to address the impact of BB particles on Sc microphysical and chemical properties for the NEP region, with a focus on the following: (i) relationships between aerosol perturbations and cloud microphysical characteristics such as droplet size distributions and drizzle rate; (ii) variations in vertical structure of cloud  $N_d$  due to BB plumes interacting with clouds; and (iii) the influence of BB aerosols on cloud droplet residual particle and cloud water composition. The results of this work have implications for general understanding of aerosol-cloud interactions, especially for regions facing growing amounts of exposure to BB emissions.

## 2. Experimental Methods

### 2.1. Center for Interdisciplinary Remotely-Piloted Aircraft Studies Twin Otter Missions

Airborne data reported in this work were collected by the Center for Interdisciplinary Remotely-Piloted Aircraft Studies Twin Otter aircraft during five separate field campaigns: (i) the first Marine Stratus/Stratocumulus Experiment (MASE I, July 2005); (ii) the second Marine Stratus/Stratocumulus Experiment (MASE II, July 2007); (iii) the Nucleation in California Experiment (NiCE, July–August 2013); (iv) the Biological and Oceanic Atmospheric Study (BOAS, July 2015); and (v) the Fog And Stratocumulus Evolution (FASE, July–August 2016) experiment. Detailed information for each campaign, including flight tracks, instruments onboard the aircraft, and measurement details such as quality control and assurance protocols are explained in Sorooshian et al. (2018). Of relevance to this work is that each flight contained aircraft soundings during which vertical profiles were obtained between the subcloud and above-cloud regions via either a spiral or slant maneuver. More detailed descriptions of soundings can be found in Sorooshian et al. (2018).

Extensive wildfire activity was present in the study region during two of the campaigns, specifically the NiCE and FASE campaigns. During NiCE, BB plumes were transported parallel to the California coastline from the California–Oregon border where there was a cluster of fires (Sorooshian et al., 2015): Big Windy, Whiskey Complex, Douglas Complex. During FASE, the source of the BB aerosols was much closer to the study domain as the Soberanes Fire (Garrapata State Park) and was only ~30 km southwest of the aircraft base in Marina, California (Schlosser et al., 2017). The criteria used to determine if an aircraft sounding during a particular flight was impacted by BB particles was if the aerosol number concentration ( $N_a$ ) measured with a Passive Cavity Aerosol Spectrometer Probe (PCASP; diameter >120 nm) exceeded  $1000\text{ cm}^{-3}$  at any altitude extending from near the surface to the free troposphere (FT). This criterion was defined based on measurements from 352 vertical soundings from more than 73 research flights without any BB influence, with the  $1000\text{ cm}^{-3}$  threshold value exceeding the mean plus three times the standard deviation of  $N_a$  during

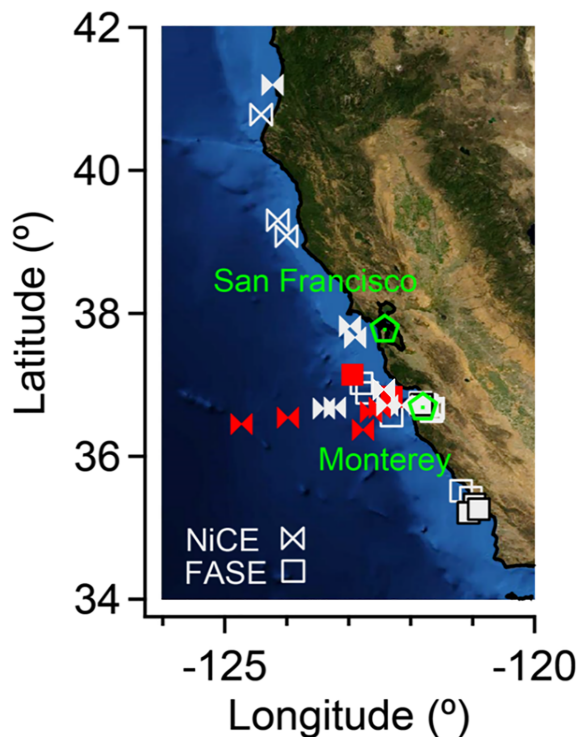


**Figure 1.** Approximate location of BB-impacted soundings during NiCE ( $n = 14$ ) and FASE ( $n = 16$ ), shown in gray. Of the mentioned soundings, eight from NiCE and five from FASE are further analyzed as case studies (Table 1), which are shown as solid gray markers; the rest are left as unfilled markers. Five soundings from NiCE and two from FASE are examined as non-BB-impacted cases (Table 1), which are shown as solid red markers.

soundings without any BB impact (Mardi et al., 2018). This criterion was shown to be reliable based on confirmation from carbon monoxide (CO) data and olfactory and visual evidence by flight scientists during the research flights. Plumes of BB particles impacted soundings in eight out of 23 and 12 out of 15 research flights during the NiCE and FASE campaigns, respectively.

Figure 1 demonstrates the spatial distribution of 30 BB-impacted soundings analyzed in this study. Traces of BB particles were observed either above or below the Sc layer. Cloud and aerosol data obtained from soundings of the other three field campaigns, in addition to non-BB-impacted soundings in NiCE and FASE, are used here to represent background conditions to contrast with BB data.

## 2.2. Cloud Measurements

Cloud droplet size distribution characteristics such as droplet number concentration ( $N_d$ ) and droplet effective radius ( $r_e$ ) were measured with a Forward Scattering Spectrometer Probe (Particle Measuring Systems, Inc., modified by Droplet Measurement Technologies, Inc.) in 20-diameter bins between 2 and 45  $\mu\text{m}$ . Rain rate ( $R$ ,  $\text{mm day}^{-1}$ ) was calculated using the size distribution of drops with diameters between 0.025 and 1.56 mm obtained from a Cloud Imaging Probe, in conjunction with documented relationships between drop size and fall velocity (e.g., Chen et al., 2012; Feingold et al., 2013). Cloud liquid water content (LWC) was measured using a PVM-100A probe (Gerber et al., 1994).

Compositional measurements were conducted two ways in clouds, specifically to characterize droplet residual particles and cloud water. The composition of cloud droplet residual particles was measured using a Compact Time-of-Flight Aerosol Mass Spectrometer (AMS; Aerodyne Research Inc.; Coggon et al., 2012) coupled to a Counter-flow Virtual Impactor

(CVI; Brechtel Mfg. Inc.) inlet. The AMS instrument measures nonrefractory constituents of particles. For the data sets used here, the cutpoint diameter of droplets sampled by the CVI was  $\sim 11 \mu\text{m}$  with a transmission efficiency that decreased with increasing droplet size mainly owing to inertial deposition (Shingler et al., 2012). Both the AMS and CVI were used in the NiCE campaign but not during FASE. Owing to uncertainties in quantifying accurate mass concentrations with the AMS downstream of the CVI (AMS-CVI), relative mass concentrations between species are the focus of the AMS-CVI data.

For the NiCE campaign, cloud water samples were collected by a modified Mohnen slotted-rod collector (Hegg & Hobbs, 1986), which was deployed manually out of aircraft during the in-cloud portion of research flights. Samples were stored in high-density polyethylene bottles in a cooler with a nominal temperature of 5°C. A detailed description of sampling process can be found in MacDonald et al. (2018). For the FASE mission, cloud water samples were collected with an axial cyclone cloud water collector (Crosbie et al., 2018) mounted on the aircraft wing. As air passes through the sampler, a helical flow pattern forms that centrifugally separates larger droplets from the flow and impacts them on the sampler's inner wall. These collected droplets get pumped to polypropylene centrifuge tubes that are capped immediately after collection and stored also at 5°C.

Three types of analyses were conducted on cloud water samples, including pH, water-soluble ionic composition, and water-soluble elemental composition. Sample pH was measured with a Thermo Scientific Orion 9110DJWP pH probe for the NiCE campaign and a Thermo Scientific Orion 8103BNUWP Ross Ultra Semi-Micro pH probe for the FASE campaign. Both probes were calibrated with 4.01 and 7.00 pH buffer solutions prior to measurements. Ionic composition was measured with the ion chromatography (IC) technique using a Thermo Scientific Dionex ICS-2100 system. Elemental composition was measured by Inductively Coupled Plasma Mass Spectrometry (Agilent 7700 Series) for NiCE and by triple quadrupole inductively coupled plasma mass spectrometry (ICP-QQQ; Agilent 8800 Series) for FASE. A list of each

**Table 1**

A summary of cloud layer-mean property ( $LWP$ ,  $N_d$ ,  $r_e$ ) values, PCASP aerosol number concentration ( $N_a$ ) above and below clouds, and cloud water (CW) pH and total air-equivalent mass concentration of a wide suite of species (see Tables S2 and S3) for soundings during NiCE and FASE with and without BB influence

Campaign	BB influence	Date	LWP ( $\text{g m}^{-2}$ )	$N_d$ ( $\text{cm}^{-3}$ )	$r_e$ ( $\mu\text{m}$ )	$N_a$ above ( $\text{cm}^{-3}$ )	$N_a$ below ( $\text{cm}^{-3}$ )	CW pH	CW mass concentration ( $\mu\text{g m}^{-3}$ )
NiCE	BB	7/29/2013	338	134	11	790	N/A	$4.21 \pm 0.28$	$29.66 \pm 14.64$
		7/29/2013	162	212	9	1,833	1,118		
		7/29/2013	197	162	10	3,279	405		
		7/29/2013	198	131	10	3,993	379		
		7/30/2013	59	119	10	511	389		
		8/2/2013	59	144	8	1,288	N/A		
		8/2/2013	71	147	8	1,707	394		
		8/2/2013	76	276	7	803	432		
	Non-BB	7/16/2013	69	29	13	102	108	$4.63 \pm 0.16$	$1.21 \pm 0.23$
		7/16/2013	180	69	13	90	123		
		7/16/2013	164	128	11	141	240		
		7/16/2013	154	75	13	328	157		
		7/24/2013	68	17	14	75	N/A		
		7/24/2013	68	17	14	75	N/A		
FASE	BB	8/4/2016	45	203	6	5,105	365	$6.85 \pm 0.22$	$11.73 \pm 10.37$
		8/4/2016	44	185	6	5,599	1,230		
		8/4/2016	42	134	7	775	207		
		8/4/2016	11	116	6	1,536	628		
		8/11/2016	107	233	7	4,008	4,489		
	Non-BB	8/5/2016	88	61	11	323	59	$4.81 \pm 0.08$	$1.71 \pm 1.21$
		8/5/2016	81	27	12	355	51		
		8/5/2016	81	27	12	355	51		

*Note.* As multiple cloud water samples may have been collected near the soundings summarized, there were more data points used in the calculation of the CW as compared to the number of soundings for the four categories below: NiCE = 8 (BB) and 6 (non-BB); FASE = 12 (BB) and 7 (non-BB). “N/A” entries in the  $N_a$  column indicate insufficient flight time below cloud base to get a reliable measurement of aerosols.

measured IC and ICP species and their limits of detection are provided in Table S1 of the supporting information. All mass concentrations from the cloud water analyses represent total air-equivalent concentrations by multiplying aqueous concentrations by the average LWC experienced during sample collection for when LWC exceeded a threshold value of  $0.02 \text{ g m}^{-3}$ .

### 2.3. Aerosol Measurements

Aerosol size distribution data were obtained with a PCASP probe (Particle Measuring Systems, Inc., modified by Droplet Measurement Technologies, Inc.), which resolved number concentrations in 20 different diameter bins between  $0.12$  and  $2.95 \mu\text{m}$  and  $0.12$  and  $3.42 \mu\text{m}$  for NiCE and FASE, respectively. CCN number concentrations were measured at 1-Hz resolution by a continuous flow streamwise thermal gradient CCN counter (Droplet Measurement Technologies; Lance et al., 2009) at a constant supersaturation of 0.2%. Aerosol parameters reported subsequently as being above cloud denote vertically averaged values from cloud top to 100 m above tops. Also, below-cloud values refer to vertically averaged values from immediately below the cloud base to the lowest possible altitude at which data were collected below bases.

### 2.4. Case Study Analysis of BB Impacts on Sc

To gain insight into the impact of BB plumes on Sc microphysical properties, soundings with the highest level of BB aerosols are compared to those with lowest level of any type of aerosols (Figure 1). More specifically, the chosen BB-impacted soundings exhibited the highest PCASP  $N_a$  concentrations above the cloud top, while the selected non-BB-impacted soundings exhibited the lowest total mass concentration among the cumulative set of species measured in cloud water samples. Relevant cloud and aerosol characteristics for these selected soundings are summarized in Table 1.

Owing to the difficulty of collecting cloud water during each sounding, the cloud water samples were collected during the horizontal flight legs in cloud near each sounding. Cloud water samples were denoted as BB-impacted if BB plumes were present either above or below the cloud layer. The same strategy was employed for the AMS-CVI measurements for which data were collected near the soundings as there was insufficient time during soundings to collect such data.



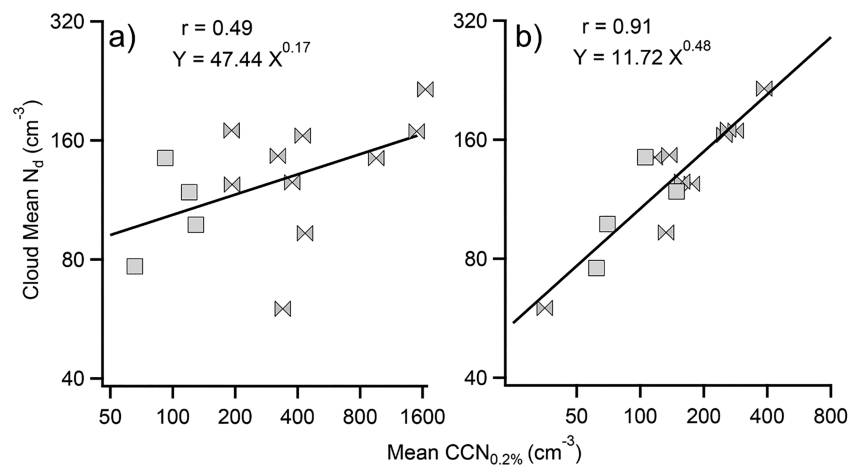


**Figure 2.** Relationship between cloud layer-mean  $N_d$  and the average  $CCN_{0.2\%}$  number concentration calculated for BB-impacted soundings (a) above cloud (between cloud top and 100 m above cloud top) and (b) below cloud base. Ten of the soundings were from NiCE (bowtie markers) and four were from FASE (square markers).

### 3. Results and Discussion

#### 3.1. $CCN-N_d$ Relationship at Cloud Base and Top

Activation of CCN into cloud droplets occurs via several mechanisms. This typically occurs via updrafts carrying aerosols at cloud base (primary activation) or by entrainment through turbulent mixing at cloud top or edge (secondary activation; Hoffmann et al., 2015; Korolev & Mazin, 1993; De Rooy et al., 2013; Slawinska et al., 2012). The relative importance for each of these mechanisms in influencing the  $N_d$  budget may vary depending on various parameters such as level of turbulence or concentration of aerosols adjacent to a cloud either aloft in the FT or below in the MBL. Our measurements provide an opportunity to examine the relative degree of importance for both mechanisms.

Figure 2 examines the relationship between cloud layer-mean  $N_d$  and  $CCN_{0.2\%}$  concentrations based on 14 soundings with BB influence.  $N_d$  exhibited an average  $\pm$  standard deviation of  $125 \pm 48 \text{ cm}^{-3}$ , while above-cloud  $CCN_{0.2\%}$  exhibited an average of  $454 \pm 493 \text{ cm}^{-3}$  as compared to  $157 \pm 97 \text{ cm}^{-3}$  below cloud. The results indicate a greater correlation between  $\log(N_d)$  and  $\log(CCN_{0.2\%})$  below cloud base ( $r = 0.91$ ;  $p < 0.01$ ) as compared to  $\log(CCN_{0.2\%})$  above cloud top ( $r = 0.49$ ;  $p = 0.08$ ); note that in our discussion of correlative relationships, that  $p < 0.05$  corresponds to statistical significance. The exponent of the power law fitted to the points is also different for each scenario, with values of 0.17 and 0.48 when using  $CCN_{0.2\%}$  above and below cloud, respectively. Past studies have quantified cloud responses to BB aerosols by computing the value of  $\partial \ln(N_d) / \partial \ln(CCN)$ , which corresponds to the power of  $X$  for the power law fit depicted in Figure 2. For the SEA region, values of this parameter based on  $CCN_{0.3\%}$  data below and above cloud were 0.45 and 0.16 (Diamond et al., 2018), respectively. These values are comparable to those shown in Figure 2 of this study based on  $CCN_{0.2\%}$  data.

As another way of examining whether above-cloud or subcloud aerosols are more influential in impacting  $N_d$ , aerosol chemical markers were compared to  $N_d$ . In the study region, aerosol composition has been extensively characterized with sulfate shown to be an excellent marker for MBL sources such as ship exhaust and marine emissions, specifically dimethylsulfide (DMS; Coggon et al., 2012; Wang et al., 2016). Nitrate and organics have been shown to be remarkably enhanced in BB airmasses (Coggon et al., 2014). Subcloud and above-cloud AMS mass concentrations of sulfate, nitrate, organics, and ammonium were compared to cloud layer-mean  $N_d$  for 13 available BB-impacted clouds during NiCE (AMS data unavailable during FASE). The subcloud concentrations of sulfate, nitrate, and organics exhibited higher linear correlations with  $N_d$  ( $r = 0.31, 0.31, 0.38$ , and  $p = 0.30, 0.35, 0.22$ , respectively) as compared to above-cloud concentrations ( $r = 0.25, -0.21, -0.02$ , and  $p = 0.43, 0.59, 0.96$ , respectively). Ammonium exhibited negative relationships with  $N_d$  (subcloud  $r = -0.25$ ,  $p = 0.63$ ; above-cloud  $r = -0.33$ ,  $p = 0.52$ ). Although none of the mentioned correlations were statistically significant (i.e.,  $p < 0.05$ ), the subcloud mass concentrations of

sulfate, nitrate, and organics were still better related to  $N_d$ , which is consistent with the conclusions derived from Figure 2.

These collective results are indicative of the greater role played by primary activation of CCN near cloud base as compared to secondary activation of CCN entrained at cloud top. This result is consistent with those of Diamond et al. (2018), who similarly reported a higher correlation between  $N_a$  and subcloud CCN concentration for the SEA region during the ObseRvations of Aerosols above CLouds and their intEractionS study. In both Diamond et al. (2018) and the current study, it is hypothesized that the increase in amount of aerosols below the cloud is due to entrainment of BB aerosols from cloud top to below the cloud. While Table 1 shows the obvious result that  $N_a$  values are much higher above cloud in BB conditions  $2,400 \text{ cm}^3$  (95% confidence interval,  $1,518\text{--}3,363 \text{ cm}^3$ ) versus non-BB conditions  $202 \text{ cm}^3$  ( $110\text{--}294 \text{ cm}^3$ ), an important result is that BB conditions also yielded much higher  $N_a$  values below cloud  $912 \text{ cm}^3$  ( $415\text{--}1,725 \text{ cm}^3$ ) versus  $123 \text{ cm}^3$  ( $73\text{--}180 \text{ cm}^3$ ). Thus, primary activation of subcloud CCN into cloud droplets is not limited to aerosols emitted within the MBL but rather can be entrained from the FT as documented in several past works (e.g., Capaldo et al., 1999; Clarke et al., 1998; Dadashazar et al., 2018; Katoshevski et al., 1999; Wood et al., 2012). Past work has examined how the variation in subcloud aerosol number concentration is related to parameters such as the gradient of CCN number concentration between vertical layers above and below cloud, boundary layer depth, and the time passed since aerosol and cloud layer have come into contact (e.g., Diamond et al., 2018; Wood et al., 2012). We compared  $\text{CCN}_{0.2\%}$  concentrations below and above cloud for the cases in Figure 2 and observed a significant correlation ( $r = 0.69$ ,  $p < 0.01$ ), with the same conclusion reached when comparing  $N_a$  below and above cloud ( $r = 0.60$ ,  $p = 0.02$ ; Figure S1). These results provide support for both the interconnectedness in CCN below and above clouds. It is critical to note though that there are factors preventing a stronger instantaneous correlation between above and below cloud BB particles such as the time dependence of entrainment (e.g., Bretherton et al., 1995; Diamond et al., 2018) and also precipitation (e.g., Wang et al., 2013).

The ease of above-cloud CCN to reach the subcloud region depends in part on how close the BB plume is to cloud top. To address this issue, we examined the relationship between both cloud layer-mean  $N_d$  and subcloud  $\text{CCN}_{0.2\%}$  concentration and the vertical distance between top of the cloud and bottom of the BB layer (referred to as AB2CT based on the terminology presented by Rajapakshe et al., 2017, to represent the gap between aerosol layer bottom to cloud top height; Figure S2). The base of the BB aerosol layer was defined as the lowest altitude of the plume where  $N_a$  exceeded  $1,000 \text{ cm}^3$  based on our previous work with the same data set (Mardi et al., 2018). A weak negative correlation was observed between cloud layer-mean  $N_d$  and AB2CT ( $r = -0.27$ ,  $p = 0.35$ ). The correlation became more negative for subcloud  $\text{CCN}_{0.2\%}$  ( $r = -0.45$ ,  $p = 0.11$ ) versus AB2CT likely due to other additional factors involved with droplet activation. These negative relationships are suggestive of the importance of BB plume proximity to cloud top for being able to impact both the MBL CCN budget.

### 3.2. $N_a$ - $N_d$ Relationship

Various physically based droplet activation schemes have established a relationship between cloud bulk microphysical properties and  $N_a$  for application in climate models (Abdul-Razzak & Ghan, 2000; Chuang et al., 1997; Nenes & Seinfeld, 2003; Simpson et al., 2014). However, several factors add to the complexity of understanding and modeling of droplet activation. A factor limiting accurate simulation of droplet activation is linked to insufficient field data, specifically for a wide range of aerosol types including BB particles. Motivated by this shortcoming, we examined how well a commonly used equation relating  $N_a$  and  $N_d$  performs with and without BB influence. Prior to doing so, it is worth noting that the two aerosol proxy variables used thus far,  $\text{CCN}_{0.2\%}$  and  $N_a$ , were related with high correlation coefficients when compared to one another below ( $r = 0.88$ ,  $p < 0.01$ ) and above cloud ( $r = 0.72$ ,  $p < 0.01$ ) for the BB cases in Figure S3.

Parameterizations of  $N_d$  based on  $N_a$  have been suggested in various formats (e.g., linear, exponential, power law) depending on the application, data set, and for various levels of required computation (Jiang et al., 2008 and references therein). One of the frequently used, yet simple, schemes is a power law relationship between cloud mean  $N_d$  and  $N_a$  at cloud base:  $N_d \sim \alpha N_a^\beta$ . This scheme is based on the assumption that for nonprecipitating clouds, droplet growth is dominated by the condensation processes and that  $N_d$  is uniform through the depth of the cloud. On the aerosol side, a homogeneous chemical composition is assumed for aerosols

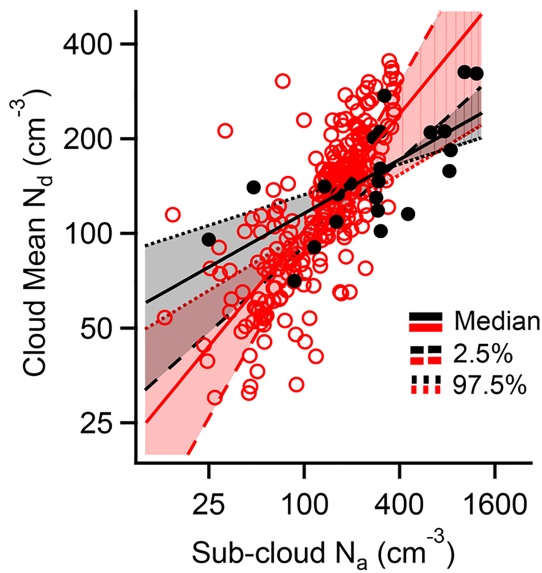


**Figure 3.** Relationship between cloud layer-mean  $N_d$  and subcloud  $N_a$  for BB-impacted soundings from NiCE and FASE (black markers with black line fit), in addition to non-BB-impacted soundings from MASE I and II, NiCE, BOAS, and FASE (red markers with red line fit). The solid line shows the median and different dashed lines show the 95% confidence interval determined via bootstrapping.

rather than considering different activation ratios for varying aerosol types in an air mass. Based on this assumption, there have been similar parameterization attempts to link the variations in cloud  $N_d$  to the variations of sulfate ( $\text{SO}_4^{2-}$ ), which is one of the most abundant aerosol species in the atmosphere (Boucher & Lohmann, 1995; Haywood & Boucher, 2000; Kiehl et al., 2000; Lohmann & Feichter, 1997; Novakov et al., 1994).

Figure 3 demonstrates the relationship between the cloud layer-mean  $N_d$  and subcloud  $N_a$  for 23 BB-impacted soundings in contrast to 266 non-BB-impacted soundings over the five campaigns. Resampling of data via bootstrapping yielded the median value (95% confidence interval) of  $\alpha = 7.73$  (1.79–26.23),  $\beta = 0.56$  (0.28–0.81), and a correlation coefficient ( $r$ ) of 0.78 (0.44–0.89) for non-BB-impacted data. These three values were as follows for BB-impacted soundings:  $\alpha = 33.25$  (12.18–65.05),  $\beta = 0.26$  (0.15–0.42), and  $r = 0.70$  (0.52–0.80). Thus, there was a significant difference in median  $\alpha$  and  $\beta$  values for the BB-impacted cases as they were outside the 95% confidence interval of values from non-BB-impacted cases. When combined, all the data in this study for BB and non-BB conditions yielded  $\alpha = 9.52$  (2.50–33.23),  $\beta = 0.50$  (0.26–0.76), and  $r = 0.76$  (0.40–0.89). Table 2 contrasts this study's values for  $\alpha$  and  $\beta$  with those from other work. The range of  $\beta$  spans from 0.26 to 0.96 with an average of 0.52, which is a range that includes  $\beta$  values from this study for BB- and non-BB-impacted conditions. For non-BB conditions in this work, the  $\beta$  value falls close to those from other studies with a similar maximum subcloud  $N_a$  value; in contrast, the value of  $\beta$  for BB conditions in this study

(0.26) is just as low as those from other studies with a much higher maximum subcloud  $N_a$  value. The relationship between  $\beta$  and the highest  $N_a$  concentration in this work (separated for BB and non-BB conditions) and for other studies is shown in Figure 4, where it is demonstrated that values adhere well to a logarithmic fit ( $r = -0.78$ ,  $p = 0.01$ ). Interestingly, if data are compared between BB and non-BB conditions from Figure 3 below the maximum  $N_a$  value recorded for non-BB conditions ( $522 \text{ cm}^{-3}$ ), the value of  $\beta$  for BB conditions (0.22) is still much lower than that for non-BB conditions.

The observed difference in the  $N_d$ - $N_a$  relationship between BB- and non-BB-impacted conditions in this work is similar to several other studies in that higher activation fractions were observed for cleaner air masses (Albrecht et al., 1995; Lu et al., 2008; Martin et al., 1994; O'Dowd et al., 2002). Factors explaining the differences in  $\beta$  could include variability in updraft speed and size distribution effects (Modini et al., 2015; Wood, 2012 and references therein). Also, it has been shown that reduced adiabaticity in clouds coincides with higher activation fractions (Braun et al., 2018), which could be an artifact of higher drizzle rates and thus

**Table 2**

A review of parameterizations provided for the relationship between  $N_d$  and  $N_a$

Region	$\alpha$	$\beta$	$r$	Highest $N_a$ ( $\text{cm}^{-3}$ )	Study
Northeast Pacific	7.73	0.56	0.78	500	This study (non-BB)
Northeast Pacific	33.25	0.26	0.70	1,800	This study (BB)
Around the British Isles and over the Atlantic near the Azores Islands	14	0.26	0.95	12,000	Raga and Jonas (1993)
Houston and the northwestern Gulf Of Mexico	33.3	0.26	0.66	11,000	Lu et al. (2008)
Vicinity of Houston, TX	36.3	0.35	N/A	10,000	Jiang et al. (2008)
Southeast Pacific	7.7	0.55	0.89	600	Terao et al. (2012)
Northeast Atlantic and North Pacific	2.75	0.73	N/A	400	O'Dowd et al. (1999) <sup>a</sup>
Northeast Pacific	1.03	0.96	0.95	500	Twohy et al. (2005) <sup>b</sup>
Pacific offshore of California, Chile, and Atlantic offshore of Namibia	13.39	0.51	0.94	700	Hegg et al. (2012) <sup>c</sup>

*Note.* All mentioned parameterizations are from studies based on in situ measurements. Reported  $\alpha$  and  $\beta$  values are either reported directly from a power law relationship or were derived from a different type of parameterization by power law fitting. Values reported in the  $r$  column belong to the original form of equations and N/A values denote that no correlation coefficient was provided by a particular study.

<sup>a</sup>Originally presented in form of  $N_d = 197 (1 - \exp(-6.13 \times 10^{-3} N_a))$ . <sup>b</sup>Originally presented in form of  $N_d = -2.2 + 1.027 N_a - 0.000837 N_a^2$ . <sup>c</sup>Originally presented in form of  $N_d = 0.72 N_a + 47$ .

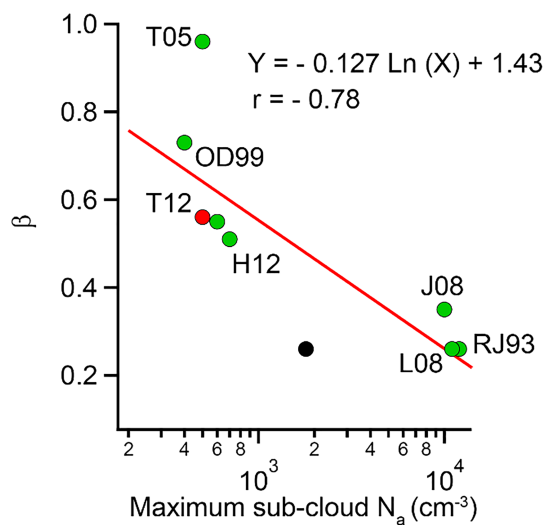


**Figure 4.** Correlation analysis between maximum subcloud  $N_a$  concentration and the  $\beta$  value obtained from the  $N_d \sim \alpha N_a^\beta$  parameterization for different studies (green markers): Hegg et al. (2012, H12), Jiang et al. (2008, J08), Lu et al. (2008, L08), O'Dowd et al. (1999, OD99), Raga and Jones (1993, RJ93), Terai et al. (2012, T12), and Twohy et al. (2005, T05). Results from the current study are included in derivation of the fitted line and are denoted for BB (black marker) and non-BB (red marker) impacted situations.

scavenging of subcloud aerosols (Duong, Sorooshian, Craven, et al., 2011; MacDonald et al., 2018). Lastly, another factor affecting the activation fraction could be aerosol hygroscopic properties, where BB aerosol are typically less CCN active than the background aerosol in the study region (Hegg et al., 2008; Hersey et al., 2009; Shingler et al., 2016). Section 3.6 addresses chemical and hygroscopic differences between BB and non-BB aerosols in more detail.

### 3.3. Vertical In-Cloud Structure of $N_d$

Various in situ observational and large eddy simulation studies reported a vertically homogeneous structure for  $N_d$  in marine Sc (Grosvenor et al., 2018 and references therein; Painemal & Zuidema, 2011). To assess the degree of vertical  $N_d$  homogeneity in the study region during periods of BB influence, vertical profiles of  $N_d$  for the selected soundings in Table 1 were examined (Figure 5). Thirteen BB-impacted clouds were compared to seven non-BB ones from NiCE and FASE.

For both campaigns, BB-impacted clouds exhibited higher vertically resolved mean and standard deviation values for  $N_d$  values along the depth of clouds as compared to non-BB-impacted clouds. Cloud layer-mean values for the mean and standard deviation of  $N_d$  were as follows: non-BB =  $71 \pm 7 \text{ cm}^{-3}$ ; BB =  $184 \pm 28 \text{ cm}^{-3}$ . Albrecht et al. (1995) similarly reported both lower absolute values and less vertical variability in  $N_d$  for a Sc sheet when exposed to cleaner maritime air (PCASP  $N_a \sim 50 \text{ cm}^{-3}$ ;  $N_d \sim 50 \text{ cm}^{-3}$ ) as compared to more polluted continental air (PCASP  $N_a \sim 1,700 \text{ cm}^{-3}$ ;  $N_d \sim 250 \text{ cm}^{-3}$ ).

There was no evidence of any type of enhancement in  $N_d$  near cloud top, which presumably would have been an indicator for secondary activation of aerosols near cloud top. This result is consistent with Figure 2 that primary activation of subcloud aerosols plays the dominant role in governing  $N_d$ .

### 3.4. $N_d$ Relationship with $r_e$ and $R$

Sections 3.1 and 3.2 examined the process of droplet activation by comparing CCN and  $N_a$  to  $N_d$ , and now, this section probes relationships between  $N_d$  and two other cloud properties for varying BB influence: cloud droplet effective radius ( $r_e$ ) and rain rate ( $R$ ). This analysis is conducted within the framework of how previous investigations have examined such relationships, with our results compared to those studies.

Figure 6a shows the relationship between  $r_e$  versus the ratio of LWP/ $N_d$  for BB versus non-BB conditions; note that all three parameters are cloud layer-mean values for consistency. Thirty BB-impacted soundings from NiCE and FASE were compared to more than 300 background non-BB-impacted soundings from MASE I and II, NiCE, BOAS, and FASE. The results do not show a significantly different response of  $r_e$  to BB particles as compared to non-BB particles. In both scenarios, a power law correlation exists between  $r_e$  and LWP/ $N_d$  with an exponent of 0.22 and 0.21 and a correlation coefficient of 0.95 and 0.91 for BB and non-BB conditions ( $p < 0.01$  for both), respectively. Various studies have applied similar parameterizations between  $r_e$  and LWC/ $N_d$  with a power law scheme, with the exponent being  $\sim 0.33$  for LWC/ $N_d$  (Jones & Slingo, 1996; Kiehl et al., 2000; Lu et al., 2008; Reid et al., 1999; Rotstain, 1999). Liu and Hallet (1997) suggested a similar parameterization and validated it by comparison with in situ collected data for non-precipitating water clouds. The values of 0.21 and 0.22 in this study are lower than 0.33 potentially owing to differences when using layer-mean values (e.g., LWP) rather than vertically resolved values (e.g., LWC), differences in the  $N_d$  (this study:  $30\text{--}328 \text{ cm}^{-3}$ ) and LWP range examined (this study:  $11\text{--}338 \text{ g m}^{-2}$ ), cloud dynamical processes, meteorology, and spatial scale of analysis (McComiskey et al., 2009).

In another study by Reid et al. (1999) for clouds partially embedded in smoky haze during the SCAR-B field project over the Amazon Basin, a power law relationship was developed with an exponent of 0.31 for LWC/ $N_d$ . As they compared the results from BB-impacted warm non-precipitating clouds to less



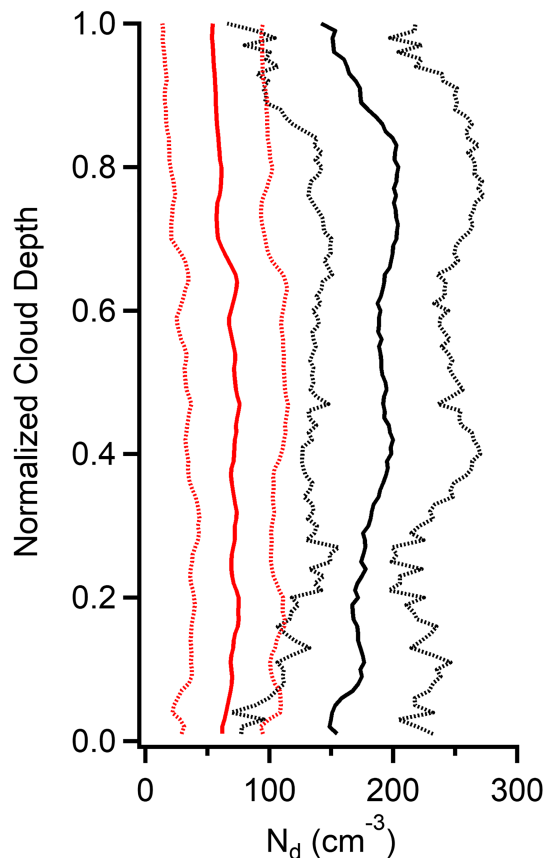


**Figure 5.** The vertical profiles of  $N_d$  plotted as a function of cloud normalized depth for the selected soundings shown in Table 1. The solid black and red lines represent average values for conditions of BB influence and minimal impact from any sources of aerosol pollution, respectively. Dashed lines indicate one standard deviation.

polluted conditions such as the east coast of the United States, they concluded that even for extreme cases of clouds impacted by BB aerosols, the parameterization provided for  $r_e$  is still valid. This is a result similar to the one obtained for our region of study as the exponent did not change much between BB and non-BB conditions.

Figure 6b demonstrates the correlation between  $R$  and the ratio of  $LWP/N_d$  and compares results from 30 BB-impacted soundings of NiCE and FASE campaigns with 232 non-BB-impacted soundings from MASE I and II, NiCE, and FASE campaigns (note that  $R$  data were unavailable during BOAS). Correlation coefficients of linear best-fit lines in log-log space were quantified based on the parameterization provided by Khairoutdinov and Kogan (2000), which demonstrated that variations in  $\log(R)$  are negatively correlated with  $\log(N_d)$  in a linear manner. Our analysis shows similar results for both scenarios (BB versus non-BB) with power law fitting; the resulting exponents were 1.06 ( $r = 0.61$ ,  $p < 0.01$ ) and 1.08 ( $r = 0.62$ ,  $p < 0.01$ ) for BB and non-BB conditions, respectively. In contrast, Comstock et al. (2004) presented a power law relationship with an exponent of 1.75 for  $LWP/N_d$  for an analysis conducted over the eastern Pacific Ocean. The differences in results can be partly attributed to factors including those outlined by Duong et al. (2011a) such as data analysis choices (e.g., calculation methods for parameters such as  $R$ , minimum  $R$  threshold) and spatial scale of data analysis.

While Sections 3.1 and 3.2 showed significant differences in aerosol- $N_d$  relationships between BB and non-BB conditions, there were no such differences when comparing  $N_d$  to  $r_e$  and  $R$  for these two conditions. It can be concluded that the existing bulk parameterizations are valid for both BB and non-BB conditions as long as  $N_d$  is captured accurately. It is cautioned though that the exponents observed in our study in Figures 6a and 6b are reduced as compared to previous work, which may at least be partly due to differences in measurement platforms, spatial scales of analysis, and how parameters were calculated (e.g., cloud-layer mean values used here).

### 3.5. Cloud Water Composition

Cloud water chemical measurements help to both identify influences from different air mass sources and shed light on cloud-gas-aerosol interaction processes like wet scavenging (Houghton, 1955; MacDonald et al., 2018; Petrenchuk & Drozdova, 1966). To further improve our understanding of BB plume impacts on marine Sc, we analyzed cloud water samples collected from BB-impacted clouds and contrasted them against non-BB-impacted ones (cases listed in Table 1). Total air-equivalent mass concentrations of measured species are reported in Table 1 for NiCE and FASE and further categorized into BB and non-BB categories. Additionally, the average mass concentration and mass fraction of measured species in BB and non-BB conditions are reported in Tables S2 and S3 for NiCE and FASE, respectively. For species including  $\text{SO}_4^{2-}$ ,  $\text{Mg}^{2+}$ ,  $\text{Ca}^{2+}$ , and  $\text{K}^+$ , the non-sea-salt portion is reported based on pure sea water ratios (Seinfeld & Pandis, 2016).

For both campaigns, the total mass concentration ( $\mu\text{g m}^{-3}$ ) of species is significantly higher for BB-impacted soundings with values of  $29.66 \pm 14.64$  and  $11.73 \pm 10.37$  from NiCE and FASE, respectively, as compared to  $1.21 \pm 0.23$  and  $1.71 \pm 1.21$  ( $\mu\text{g m}^{-3}$ ) for non-BB-impacted samples. This equates to an approximate increase in total mass concentration of 2,351% for NiCE and 586% for FASE. The enhancement in mass loading in BB conditions is partly attributed to higher concentrations of aerosol and gaseous species in BB plumes that enter into clouds through either cloud top or cloud base. The similarity in mass loadings between NiCE and FASE during non-BB conditions is expected as the predominant sources impacting the region in the absence of wildfires is similar between different years in the summer months. However, the difference in

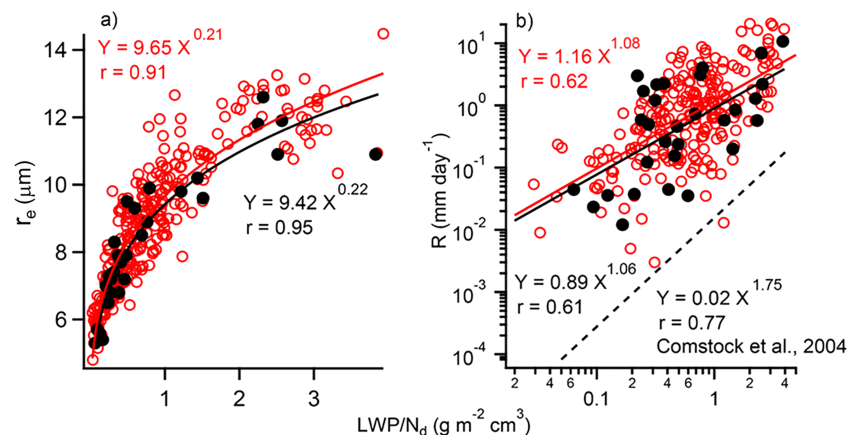


**Figure 6.** (a) Correlation analysis between  $r_e$  and  $\text{LWP}/N_d$  for BB-impacted soundings from NiCE and FASE (black markers) as compared to non-BB-impacted soundings from MASE I and II, NiCE, BOAS, and FASE (red markers). (b) Same as (a) except with  $R$  in place of  $r_e$ . Power law fits are provided for both panels separately for BB-impacted and non-BB-impacted soundings, with that of Comstock et al. (2004) additionally added as a dashed line in (b).

mass concentrations between NiCE and FASE during BB conditions can be explained by some combination of factors related to the fire characteristics (fuel type, flame condition, fire strength) and transport pathway from the fire source to the sampled clouds as during NiCE the fires were farther to the north while in FASE the fire source was very close to the base of operations in Marina.

Figures 7 and 8 show the relative mass fractions of species in BB and non-BB-impacted cloud water samples during NiCE and FASE, respectively. For the FASE campaign, the mass fraction of non-sea-salt species is much higher for BB-impacted cloud water samples as compared to the non-BB ones. This was especially the case for  $\text{NO}_3^-$ , which is associated with BB particles in the study region (Prabhakar et al., 2014). In sharp contrast, during NiCE, the total mass concentrations of species derived from sea salt (e.g.,  $\text{Na}^+$ ,  $\text{Cl}^-$ ) were more enhanced for BB conditions; in fact, when excluding  $\text{Na}^+$  and  $\text{Cl}^-$  from the analysis, the total mass concentration of species in FASE BB periods ( $7.57 \mu\text{g m}^{-3}$ ) exceeded that during NiCE ( $5.98 \mu\text{g m}^{-3}$ ). It is uncertain as to why sea salt mass was so high ( $\text{Na}^+ + \text{Cl}^- = 23.64 \mu\text{g m}^{-3}$ ) during BB periods in NiCE, and it is very likely that this was only a coincidence without any relationship between the presence of a BB plume aloft and higher sea salt fluxes. During both campaigns, regardless of BB or non-BB conditions, the  $\text{Cl}^-:\text{Na}^+$  mass concentration ratios were close to the expected ratio for pure sea salt (1.81): NiCE =  $1.71 \pm 0.12$  (BB) and  $1.65 \pm 0.40$  (non-BB); FASE =  $1.76 \pm 0.36$  (BB) and  $1.76 \pm 0.04$  (non-BB). The slight reductions as compared to sea salt are likely attributed to well-documented chloride depletion reactions owing to inorganic and organic acids that are ubiquitous in the study region (Braun et al., 2017). Future research is warranted to identify if the extent of chloride depletion observed here was minor owing to the abundance of surface area provided by crustal material to accommodate acidic gases, thereby relieving sea salt particles.

A noteworthy difference between BB and non-BB conditions was the concentration increase in crustally derived species (e.g.,  $\text{Ca}^{2+}$ , Si, and  $\text{Mg}^{2+}$ ) for the former, which was especially pronounced during FASE. During FASE,  $\text{Ca}^{2+}$  and  $\text{Mg}^{2+}$  exhibited a significant correlation ( $r = 0.92$ ,  $p < 0.01$ ). This suggests a similar source for  $\text{Ca}^{2+}$  and  $\text{Mg}^{2+}$  in FASE samples, which is most probably terrestrial dust; this is confirmed by their significant correlation with Si ( $r = 0.64$ ,  $p = 0.03$ ), which is a crustal tracer in the study region (Wang et al., 2014). Soil dust can be entrained into buoyant BB plumes, which is common across the western United States (Schlosser et al., 2017 and references therein). The proximity of the FASE fire to the sampling areas may be a reason for why the chemical signature of crustal matter was more evident than NiCE when the absolute concentrations of the same crustal species were lower by an order of magnitude.

The enhancement of crustal tracer species in FASE BB plumes can explain why the average pH in BB-impacted cloud water was significantly higher ( $6.85 \pm 0.22$ ) than non-BB-impacted samples ( $4.81 \pm 0.08$ ).

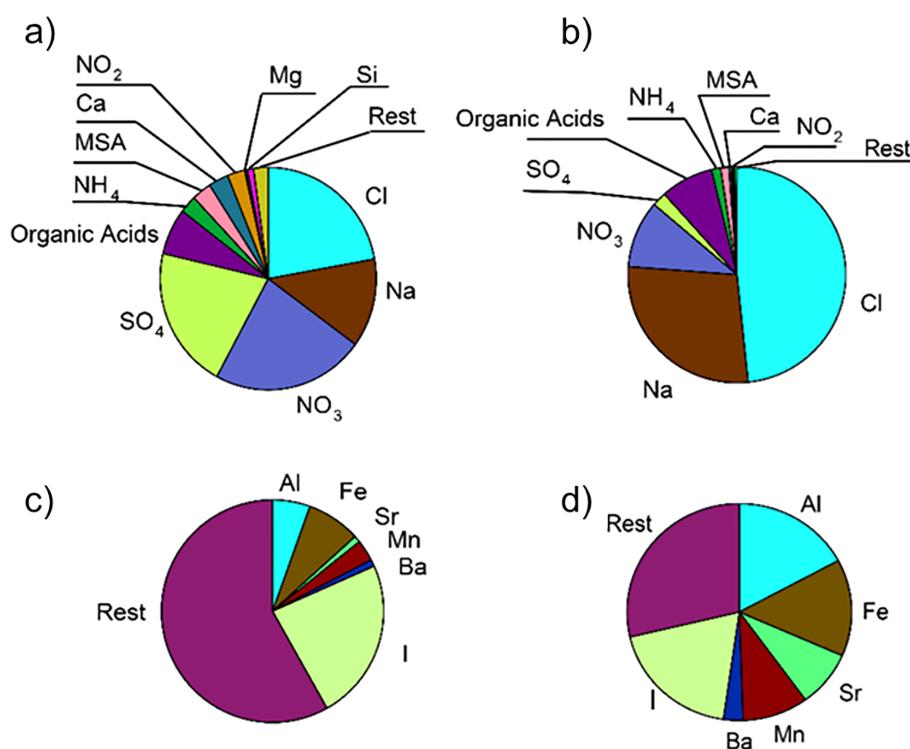


**Figure 7.** Average mass fraction of various species in collected cloud water samples during the NiCE campaign based on the selected cases in Table 1. Panel (a) demonstrates the average mass ratios obtained from non-BB-impacted samples and panel (b) shows results for BB-impacted samples. Panels (c) and (d) are expansions of the portion denoted as “Rest” in panels (a) and (b), respectively. Species which contribute to the slice labeled as the “Rest” in panels (c-d) are reported in Table S4. Average pH and total mass concentrations for BB and non-BB-impacted soundings of each campaign are reported in Table 1.

Such a difference was not observed in the pH of samples collected during NiCE with values of  $4.21 \pm 0.28$  and  $4.63 \pm 0.16$  for BB and non-BB-impacted samples, respectively. Higher pH values typically coincide with enrichment of crustal species, which increase the alkalinity of cloud water samples as observed in other regions (e.g., Loye-pilot & Morelli, 1988; Rhoades et al., 2010; Schwikowski et al., 1995; Sorooshian, Shingler, et al., 2013; Williams & Melack, 1991).

Of note is that a series of organic acids (oxalate, acetate, formate, glycolate, succinate, adipate, maleate, pyruvate) were collectively higher in concentration by an order of magnitude in BB-impacted clouds during NiCE ( $1.68 \mu\text{g m}^{-3}$ ) versus FASE ( $0.21 \mu\text{g m}^{-3}$ ), whereas their respective non-BB levels were much lower ( $0.04\text{--}0.07 \mu\text{g m}^{-3}$  for FASE and NiCE, respectively). During NiCE, the additional transport time of the BB plumes to the points of measurement may have aided in organic acid formation owing to the lengthy chemistry required to produce such species from gaseous volatile organic compound precursors (Mardi et al., 2018). Furthermore, there could have been recondensation of organic species following their evaporation after aging was allowed to ensue, which has been shown in other studies (e.g., Akagi et al., 2012; Grieshop et al., 2009).

As further support for aging leading to more organic acids during the NiCE BB periods, Figure 9 shows the spatial distribution of two relevant ratios from the AMS instrument during one particular flight when the plume was traced from near the source at southern Oregon toward the central coast of California: the fraction of organic at  $m/z$  44 ( $f_{44}$ ) and of organic at  $m/z$  60 ( $f_{60}$ ). The former ratio ( $f_{44}$ ) increased with plume transport indicating that the plume aged quickly, yielding a relatively high amount of oxygenated organic material such as organic acids (Ng et al., 2011). The reduction of ( $f_{60}$ ) along the plume track showed that levoglucosan, a marker for fresh BB emissions (Alfarra et al., 2007), decreased relatively quickly and that consequently, primary organic aerosol near the source was replaced by secondary organic aerosol farther

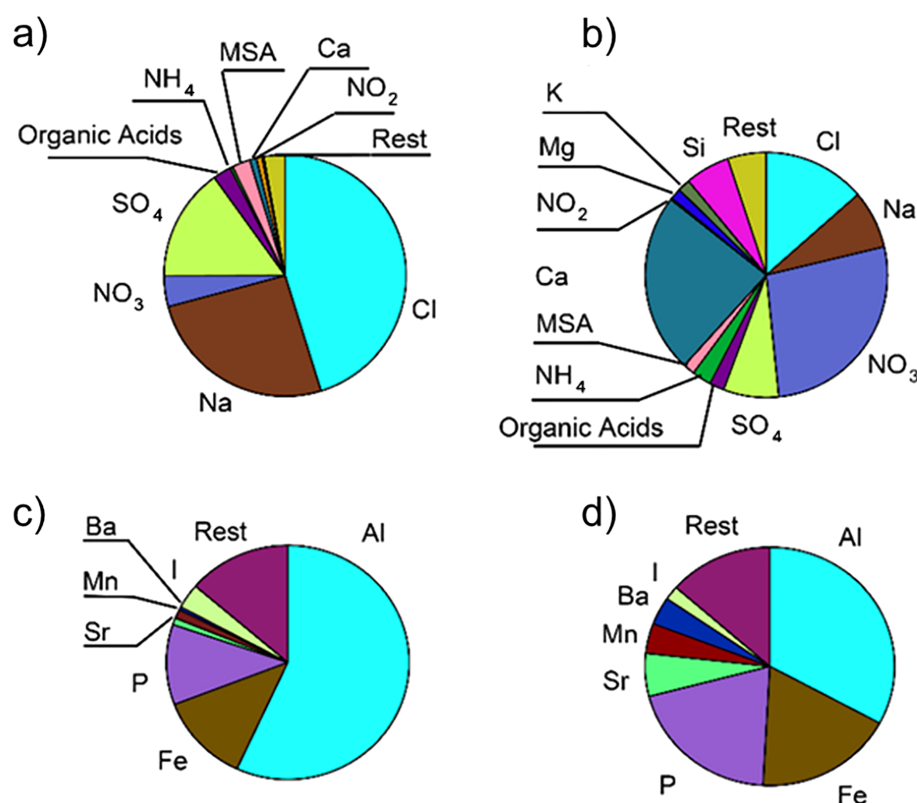


Figure 8. Same as Figure 7, but for the FASE campaign.

downwind. It is noted that levoglucosan has been observed to decrease when exposed to hydroxy radicals (Hennigan et al., 2010) and possibly due to dilution.

### 3.6. Cloud Droplet Residual Particle Composition

The relative mass concentrations of nonrefractory aerosol constituents measured with the CVI-AMS technique are shown in Figure 10 for non-BB and BB-impacted soundings from NiCE (unavailable during FASE). The main difference is that, relative to non-BB conditions, BB influenced samples coincided with an increase in the organic fraction (95% confidence intervals: BB = 64–66%, non-BB = 27–32%) and a decrease in the mass fraction of  $\text{SO}_4^{2-}$  (BB = 19–21%, non-BB = 50–55%). Nitrate and  $\text{NH}_4^+$  mass fractions exhibited less change between the two types of conditions (BB/non-BB):  $\text{NO}_3^-$  = 6–7%/4–6%;  $\text{NH}_4^+$  = 8–9%/11–15%. Numerous studies have reported that BB plumes are enriched with organic constituents (e.g., Akagi et al., 2012; Duong, Sorooshian, & Feingold, 2011; Formenti et al., 2003; Gao et al., 2003; Reid et al., 1998), and thus, the remarkable enhancement in the organic mass fraction in BB-impacted clouds is expected. The relative importance of  $\text{SO}_4^{2-}$  decreased in BB-impacted clouds simply due to the usual sources in the boundary layer (DMS, shipping) being outweighed by the injection of organics. While there was significant enhancement of  $\text{NO}_3^-$  in the regional BB plumes, the heating of the CVI counter-flow promotes repartitioning of  $\text{NO}_3^-$  back to the gas phase as has been documented in past work (e.g., Hayden et al., 2008). While these results demonstrate the impact of BB plumes on droplet residual chemistry, it is noted that there are differences with the cloud water results for the following reasons: (i) The AMS is limited to submicrometer aerosols unlike cloud water collection; (ii) semi-volatile species are vulnerable to evaporation in the heated counterflow of the CVI inlet (and thus would not be sampled by the AMS) unlike cloud water collection; and (iii) the cloud water collector can sample constituents such as sea salt and an assortment of crustal elements that the AMS cannot.

As hinted to before in the discussion of CCN activation ratios, aerosol compositional effects can potentially be important for CCN activity for the regional-scale BB events sampled in this work. Martin et al. (1994) cited



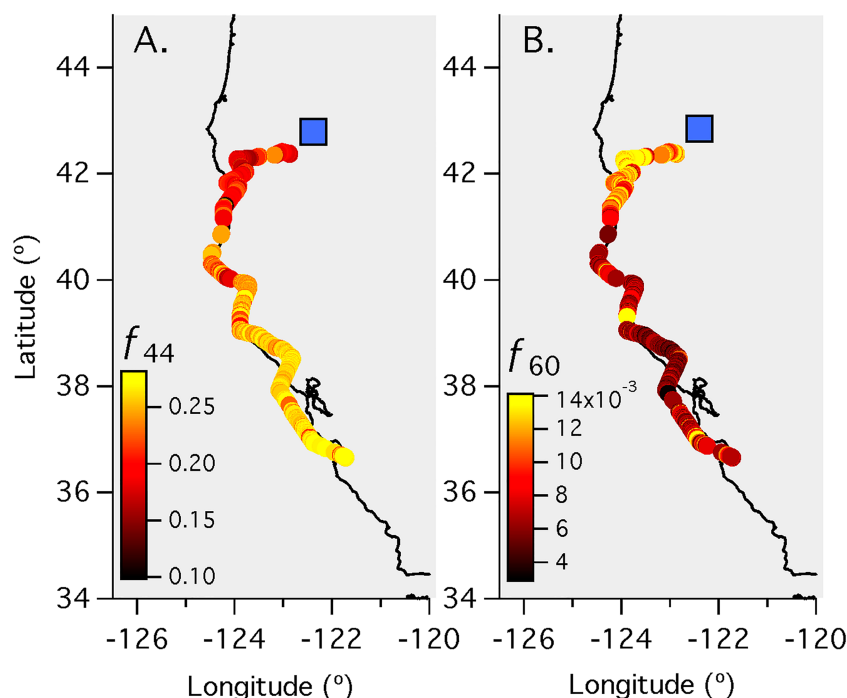


**Figure 9.** Twin Otter flight path colored by (A) the fraction of organic at  $m/z$  44 ( $f_{44}$ ) and (B) the fraction of organic at  $m/z$  60 ( $f_{60}$ ) for NiCE Research Flight 17 on 30 July 2013. Shown are samples containing smoke from the cluster of fires in southern Oregon (blue square). Greater  $f_{44}$  is an indication of oxidized organic aerosol (largely associated with organic acids, Ng et al., 2011), whereas greater  $f_{60}$  indicates a higher fraction of levoglucosan, a marker for fresh BB emissions (Alfarra et al., 2007).

differences in aerosol composition in explaining why the activation ratio of continental aerosols was different than marine aerosols. Similar reasoning of higher CCN activity for more water-soluble aerosol types has been provided by other studies in our study region based on ship-board measurements (Wonaschuetz et al., 2013) and modeling studies (Sanchez et al., 2016). As shown by the CVI-AMS results and confirmed by previous studies in the same region, BB air masses have much higher concentrations of organics (Crosbie et al., 2016; Mardi et al., 2018; Maudlin et al., 2015), which have reduced hygroscopicity as compared to aerosol less enriched with organics (e.g., Hersey et al., 2009; Shingler et al., 2016). While it is difficult to attribute the relative importance of chemical effects to the reduced activation fraction for BB conditions in this study, it is at least one plausible factor that may have played a role.

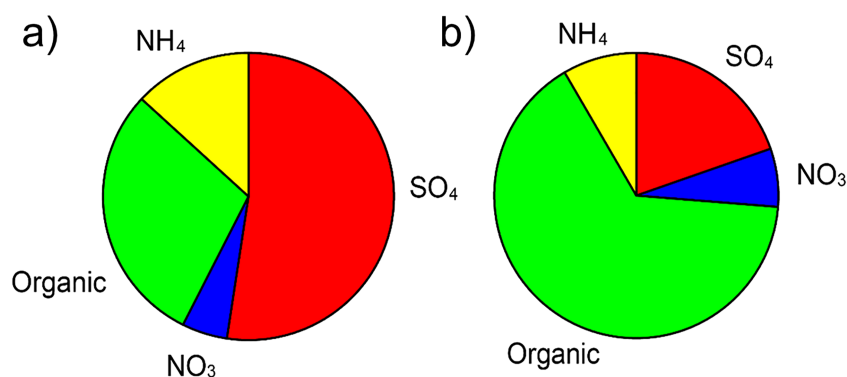


**Figure 10.** Average mass fraction of species measured by an AMS coupled to a CVI inlet during the NiCE campaign for (a) clouds with minimal influence from aerosols and (b) BB-impacted clouds. These data are based on the selected cases summarized in Table 1.

## 4. Conclusions

This study represents the second part of a two-part paper series examining BB plumes off the California coast. The first study (Mardi et al., 2018) characterized plume properties, while this study examined interactions between plumes and Sc clouds. The main results of this study are as follows:

1. Stronger relationships between subcloud aerosol properties with cloud layer-mean  $N_d$  values and the lack of a clear vertical enhancement in  $N_d$  at cloud top indicated that primary activation of subcloud CCN was more important in governing  $N_d$  values than secondary activation of CCN entrained at cloud top. The data results indicate that the MBL BB aerosols likely were sourced to a large extent from the FT at some point. An instantaneous correlation between above- and below-cloud BB particles is complicated though by factors such as the time dependence of entrainment and also precipitation.
2. BB-impacted clouds exhibited higher vertically resolved mean and standard deviation values for  $N_d$  values along the depth of clouds as compared to non-BB-impacted clouds.
3. Lower CCN activation fractions were observed for BB-impacted clouds as compared to non-BB clouds owing at least to some extent to less hygroscopic aerosol constituents.
4. Relationships between  $N_d$  and either  $r_e$  or  $R$  were similar regardless of the level of influence from BB plumes, indicating that parameterizations relating these cloud properties can handle both BB and non-BB conditions as long as the  $N_d$  value is known.
5. Cloud water data show that in FASE there was more enhancement in crustal tracer species due likely to the proximity of the fires to the sampling area, which was more conducive to measurement of coarse dust aerosols entrained in the buoyant BB plumes. Consequently, pH values were much more enhanced in BB-impacted clouds during FASE. In contrast during NiCE, higher overall mass concentrations of organic acids are thought to have arisen due to longer transport times that promoted more production of these species.
6. Cloud droplet residual particle composition results reveal significant enhancements in the relative amount of organics during BB periods at the expense of sulfate, while nitrate and ammonium remain relatively similar in their mass fractions.

The results of this study are useful in terms of contrasting with other regions where BB plumes have the ability to impact cloud properties. In particular, impacts of BB plumes on cloud composition are generally understudied and important for future research as such modifications have an impact on both aqueous chemistry (e.g., Keene et al., 2015; Sorooshian, Wang, et al., 2013) and ecosystems after wet deposition of nutrients and contaminants (e.g., Galloway et al., 2004; Meskhidze et al., 2005).

## Acknowledgments

All data used in this work can be found on the Figshare database (Sorooshian et al., 2018; [https://figshare.com/articles/A\\_Multi-Year\\_Data\\_Set\\_on\\_Aerosol-Cloud-Precipitation-Meteorology\\_Interactions\\_for\\_Marine\\_Stratocumulus\\_Clouds/5099983](https://figshare.com/articles/A_Multi-Year_Data_Set_on_Aerosol-Cloud-Precipitation-Meteorology_Interactions_for_Marine_Stratocumulus_Clouds/5099983)). This work was funded by Office of Naval Research grants N00014-10-1-0811, N00014-11-1-0783, N00014-10-1-0200, N00014-04-1-0118, and N00014-16-1-2567. This work was also partially supported by NASA grant 80NSSC19K0442 in support of the ACTIVATE Earth Venture Suborbital-3 (EVS-3) investigation, which is funded by NASA's Earth Science Division and managed through the Earth System Science Pathfinder Program Office.

## REFERENCES

- Abdul-Razzak, H., & Ghan, S. J. (2000). A parameterization of aerosol activation 2. Multiple aerosol types. *Journal of Geophysical Research*, 105(d5), 6837–6844. <https://doi.org/10.1029/1999jd901161>
- Akagi, S. K., Craven, J. S., Taylor, J. W., McMeeking, G. R., Yokelson, R. J., Burling, I. R., et al. (2012). Evolution of trace gases and particles emitted by a chaparral fire in California. *Atmospheric Chemistry and Physics*, 12(3), 1397–1421. <https://doi.org/10.5194/acp-12-1397-2012>
- Albrecht, B. A., Bretherton, C. S., Johnson, D., Scubert, W. H., & Frisch, A. S. (1995). The Atlantic stratocumulus transition experiment—ASTEX. *Bulletin of the American Meteorological Society*, 76(6), 889–904. [https://doi.org/10.1175/1520-0477\(1995\)076<0889:taste>2.0.co;2](https://doi.org/10.1175/1520-0477(1995)076<0889:taste>2.0.co;2)
- Alfarra, M. R., Prevot, A. S. H., Szidat, S., Sandradewi, J., Weimer, S., Lanz, V. A., et al. (2007). Identification of the mass spectral signature of organic aerosols from wood burning emissions. *Environmental Science & Technology*, 41(16), 5770–5777. <https://doi.org/10.1021/es062289b>
- Barbero, R., Abatzoglou, J. T., Larkin, N. K., Kolden, C. A., & Stocks, B. (2015). Climate change presents increased potential for very large fires in the contiguous United States. *International Journal of Wildland Fire*, 24(7), 892–899. <https://doi.org/10.1071/wf15083>
- Boucher, O., & Lohmann, U. (1995). The sulfate-CCN-cloud albedo effect—A sensitivity study with 2 general-circulation models. *Tellus Series B-Chemical and Physical Meteorology*, 47(3), 281–300. <https://doi.org/10.1034/j.1600-0889.47.issue3.1.x>
- Braun, R. A., Dadashazar, H., Macdonald, A. B., Aldhaif, A. M., Maudlin, L. C., Crosbie, E., et al. (2017). Impact of wildfire emissions on chloride and bromide depletion in marine aerosol particles. *Environmental Science and Technology*, 51(16), 9013–9021. <https://doi.org/10.1021/acs.est.7b02039>
- Braun, R. A., Dadashazar, H., Macdonald, A. B., Crosbie, E., Jonsson, H. H., Woods, R. K., et al. (2018). Cloud adiabaticity and its relationship to marine stratocumulus characteristics over the northeast Pacific Ocean. *Journal of Geophysical Research: Atmospheres*, 123(24), 13790–13806. <https://doi.org/10.1029/2018jd029287>
- Bretherton, C. S., Austin, P., & Siems, S. T. (1995). Cloudiness and marine boundary layer dynamics in the ASTEX Lagrangian experiments. Part II: Cloudiness, drizzle, surface fluxes, and entrainment. *Journal of the Atmospheric Sciences*, 52(16), 2724–2735. [https://doi.org/10.1175/1520-0469\(1995\)052<2724:CAMBLD>2.0.CO;2](https://doi.org/10.1175/1520-0469(1995)052<2724:CAMBLD>2.0.CO;2)

- Brioude, J., Cooper, O. R., Feingold, G., Trainer, M., Freitas, S. R., Kowal, D., et al., (2009). Effect of biomass burning on marine stratocumulus clouds off the California coast. *Atmospheric Chemistry and Physics*, 9(22), 8841–8856. <https://doi.org/10.5194/acp-9-8841-2009>
- Capaldo, K. P., Kasibhatla, P., & Pandis, S. N. (1999). Is aerosol production within the remote marine boundary layer sufficient to maintain observed concentrations? *Journal of Geophysical Research-Atmospheres*, 104(D3), 3483–3500. <https://doi.org/10.1029/1998jd100080>
- Chen, T., Rossow, W. B., & Zhang, Y. C. (2000). Radiative effects of cloud-type variations. *Journal of Climate*, 13(1), 264–286. [https://doi.org/10.1175/1520-0442\(2000\)013<0264:reoctv>2.0.co;2](https://doi.org/10.1175/1520-0442(2000)013<0264:reoctv>2.0.co;2)
- Chen, Y.-C., Christensen, M. W., Xue, L., Sorooshian, A., Stephens, G. L., Rasmussen, R. M., & Seinfeld, J. H. (2012). Occurrence of lower cloud albedo in ship tracks. *Atmospheric Chemistry and Physics*, 12(17), 8223–8235. <https://doi.org/10.5194/acp-12-8223-2012>
- Chuang, C. C., Penner, J. E., Taylor, K. E., Grossman, A. S., & Walton, J. J. (1997). An assessment of the radiative effects of anthropogenic sulfate. *Journal of Geophysical Research-Atmospheres*, 102(d3), 3761–3778. <https://doi.org/10.1029/96jd03087>
- Clarke, A. D., Varner, J. L., Eisele, F., Mauldin, R. L., Tanner, D., & Litchy, M. (1998). Particle production in the remote marine atmosphere: Cloud outflow and subsidence during ACE 1. *Journal of Geophysical Research-Atmospheres*, 103(D13), 16397–16409. <https://doi.org/10.1029/97jd02987>
- Coggon, M. M., Sorooshian, A., Wang, Z., Craven, J. S., Metcalf, A. R., Lin, J. J., et al. (2014). Observations of continental biogenic impacts on marine aerosol and clouds off the coast of California. *Journal of Geophysical Research: Atmospheres*, 119, 6724–6748. <https://doi.org/10.1002/2013jd021228>
- Coggon, M. M., Sorooshian, A., Wang, Z., Metcalf, A. R., Frossard, A. A., Lin, J. J., (2012). Ship impacts on the marine atmosphere: Insights into the contribution of shipping emissions to the properties of marine aerosol and clouds. *Atmospheric Chemistry and Physics*, 12(18), 8439–8458. <https://doi.org/10.5194/acp-12-8439-2012>
- Comstock, K. K., Wood, R., Yuter, S. E., & Bretherton, C. S. (2004). Reflectivity and rain rate in and below drizzling stratocumulus. *Quarterly Journal of The Royal Meteorological Society*, 130(603, b), 2891–2918. <https://doi.org/10.1256/qj.03.187>
- Costantino, L., & Bréon, F. M. (2010). Analysis of aerosol-cloud interaction from multi-sensor satellite observations. *Geophysical Research Letters*, 37, L11801 <https://doi.org/10.1029/2009gl041828>
- Costantino, L., & Bréon, F. M. (2013). Aerosol indirect effect on warm clouds over south-east Atlantic, from co-located MODIS and CALIPSO observations. *Atmospheric Chemistry and Physics*, 13(1), 69–88. <https://doi.org/10.5194/acp-13-69-2013>
- Crosbie, E., Brown, M. D., Shook, M., Ziemba, L., Moore, R. H., Shingler, T., et al. (2018). Development and characterization of a high-efficiency, aircraft-based axial cyclone cloud water collector. *Atmospheric Measurement Techniques*, 11(9), 5025–5048. <https://doi.org/10.5194/amt-11-5025-2018>
- Crosbie, E., Wang, Z., Sorooshian, A., Chuang, P. Y., Craven, J. S., Coggon, M. M., et al. (2016). Stratocumulus cloud clearings and notable thermodynamic and aerosol contrasts across the clear-cloudy interface. *Journal of The Atmospheric Sciences*, 73(3), 1083–1099. <https://doi.org/10.1175/JAS-D-15-0137.1>
- Dadashazar, H., Braun, R. A., Crosbie, E., Chuang, P. Y., Woods, R. K., Jonsson, H. H., & Sorooshian, A. (2018). Aerosol characteristics in the entrainment interface layer in relation to the marine boundary layer and free troposphere. *Atmospheric Chemistry and Physics*, 18(3), 1495–1506. <https://doi.org/10.5194/acp-18-1495-2018>
- Dadashazar, H., Ma, L., & Sorooshian, A. (2019). Sources of pollution and interrelationships between aerosol and precipitation chemistry at a central California site. *Science of The Total Environment*, 651(Pt 2), 1776–1787. <https://doi.org/10.1016/j.scitotenv.2018.10.086>
- Das, S., Harshvardhan, H., Bian, H., Chin, M., Curci, G., Protonotariou, A. P., et al. (2017). Biomass burning aerosol transport and vertical distribution over the south African-Atlantic region. *Journal of Geophysical Research: Atmospheres*, 122, 6391–6415. <https://doi.org/10.1002/2016jd026421>
- De Rooy, W. C., Bechtold, P., Froehlich, K., Hohenegger, C., Jonker, H., Mironov, D., et al. (2013). Entrainment and detrainment in cumulus convection: an overview. *Quarterly Journal of The Royal Meteorological Society*, 139(670, a), 1–19. <https://doi.org/10.1002/qj.1959>
- Dennison, P. E., Brewer, S. C., Arnold, J. D., & Moritz, M. A. (2014). Large wildfire trends in the western United States, 1984–2011. *Geophysical Research Letters*, 41, 2928–2933. <https://doi.org/10.1002/2014gl059576>
- Diamond, M. S., Dobracki, A., Freitag, S., Griswold, J. D. S., Heikkilä, A., Howell, S. G., et al. (2018). Time-dependent entrainment of smoke presents an observational challenge for assessing aerosol-cloud interactions over the southeast Atlantic Ocean. *Atmospheric Chemistry and Physics*, 18(19), 14623–14636. <https://doi.org/10.5194/acp-18-14623-2018>
- Duong, H. T., Sorooshian, A., Craven, J. S., Hersey, S. P., Metcalf, A. R., Zhang, X., et al. (2011). Water-soluble organic aerosol in the Los Angeles basin and outflow regions: Airborne and ground measurements during the 2010 CALNEX field campaign. *Journal of Geophysical Research-Atmospheres*, 116. <https://doi.org/10.1029/2011jd016674>
- Duong, H. T., Sorooshian, A., & Feingold, G. (2011). Investigating potential biases in observed and modeled metrics of aerosol-cloud-precipitation interactions. *Atmospheric Chemistry and Physics*, 11(9), 4027–4037. <https://doi.org/10.5194/acp-11-4027-2011>
- Feingold, G., McComiskey, A., Rosenfeld, D., & Sorooshian, A. (2013). On the relationship between cloud contact time and precipitation susceptibility to aerosol. *Journal of Geophysical Research: Atmospheres*, 118, 10544–10554. <https://doi.org/10.1002/jgrd.50819>
- Flannigan, M. D., Stocks, B. J., & Wotton, B. M. (2000). Climate change and forest fires. *Science of the Total Environment*, 262(3), 221–229. [https://doi.org/10.1016/s0048-9697\(00\)00524-6](https://doi.org/10.1016/s0048-9697(00)00524-6)
- Formenti, P., Elbert, W., Maenhaut, W., Haywood, J., Osborne, S., & Andreae, M. O. (2003). Inorganic and carbonaceous aerosols during the southern African regional science initiative (safari 2000) experiment: Chemical characteristics, physical properties, and emission data for smoke from African biomass burning. *Journal of Geophysical Research-Atmospheres*, 108(d13). <https://doi.org/10.1029/2002jd002408>
- Galloway, J. N., Dentener, F. J., Capone, D. G., Boyer, E. W., Howarth, R. W., Seitzinger, S. P., et al. (2004). Nitrogen cycles: Past, present, and future. *Biogeochemistry*, 70(2), 153–226. <https://doi.org/10.1007/s10533-004-0370-0>
- Gao, S., Hegg, D. A., Hobbs, P. V., Kirchstetter, T. W., Magi, B. I., & Sadilek, M. (2003). Water-soluble organic components in aerosols associated with savanna fires in southern Africa: identification, evolution, and distribution. *Journal of Geophysical Research-Atmospheres*, 108(d13). <https://doi.org/10.1029/2002jd002324>
- Gerber, H., Arends, B. G., & Ackerman, A. S. (1994). New microphysics sensor for aircraft use. *Atmospheric Research*, 31(4), 235–252. [https://doi.org/10.1016/0169-8095\(94\)90001-9](https://doi.org/10.1016/0169-8095(94)90001-9)
- Grieshop, A. P., Logue, J. M., Donahue, N. M., & Robinson, A. L. (2009). Laboratory investigation of photochemical oxidation of organic aerosol from wood fires I: Measurement and simulation of organic aerosol evolution. *Atmospheric Chemistry and Physics*, 9(4), 1263–1277. <https://doi.org/10.5194/acp-9-1263-2009>

- Grosvenor, D. P., Sourdeval, O., Zuidema, P., Ackerman, A., Alexandrov, M. D., Bennartz, R., et al. (2018). Remote sensing of droplet number concentration in warm clouds: A review of the current state of knowledge and perspectives. *Reviews of Geophysics*, 56(2), 409–453. <https://doi.org/10.1029/2017rg000593>
- Hallar, A. G., Molotch, N. P., Hand, J. L., Livneh, B., Mccubbin, I. B., Petersen, R., et al. (2017). Impacts of increasing aridity and wildfires on aerosol loading in the intermountain western US. *Environmental Research Letters*, 12(1). <https://doi.org/10.1088/1748-9326/aa510a>
- Harrison, E. F., Minnis, P., Barkstrom, B. R., Ramanathan, V., Cess, R. D., & Gibson, G. G. (1990). Seasonal variation of cloud radiative forcing derived from the Earth radiation budget experiment. *Journal of Geophysical Research-Atmospheres*, 95(d11), 18687–18703. <https://doi.org/10.1029/jd095id11p18687>
- Hartmann, D. L., & Short, D. A. (1980). On the use of earth radiation budget statistics for studies of clouds and climate. *Journal of The Atmospheric Sciences*, 37(6), 1233–1250. [https://doi.org/10.1175/1520-0469\(1980\)037<1233:otuoer>2.0.co;2](https://doi.org/10.1175/1520-0469(1980)037<1233:otuoer>2.0.co;2)
- Hayden, K. L., Macdonald, A. M., Gong, W., Toom-Sauntry, D., Anlauf, K. G., Leithead, A., et al. (2008). Cloud processing of nitrate. *Journal of Geophysical Research-Atmospheres*, 113(d18). <https://doi.org/10.1029/2007jd009732>
- Haywood, J., & Boucher, O. (2000). Estimates of the direct and indirect radiative forcing due to tropospheric aerosols: A review. *Reviews of Geophysics*, 38(4), 513–543. <https://doi.org/10.1029/1999rg000078>
- Hegg, D. A., Covert, D. S., & Jonsson, H. H. (2008). Measurements of size-resolved hygroscopicity in the California coastal zone. *Atmospheric Chemistry and Physics*, 8(23), 7193–7203.
- Hegg, D. A., Covert, D. S., Jonsson, H. H., & Woods, R. K. (2012). A simple relationship between cloud drop number concentration and precursor aerosol concentration for the regions of earth's large marine stratocumulus decks. *Atmospheric Chemistry and Physics*, 12(3), 1229–1238. <https://doi.org/10.5194/acp-12-1229-2012>
- Hegg, D. A., & Hobbs, P. V. (1986). *Studies of the mechanisms and rate with which nitrogen species are incorporated into cloud water and precipitation, Second Annual Report on Project CAPA-21-80 to the Coordinating Research Council.*
- Hennigan, C. J., Sullivan, A. P., Collett, J. L., & Robinson, A. L. (2010). Levoglucosan stability in biomass burning particles exposed to hydroxyl radicals. *Geophysical Research Letters*, 37.
- Herman, G. F., Wu, M. L. C., & Johnson, W. T. (1980). The effect of clouds on the earth's solar and infrared radiation budgets. *Journal of The Atmospheric Sciences*, 37(6), 1251–1261. [https://doi.org/10.1175/1520-0469\(1980\)037<1251:teocot>2.0.co;2](https://doi.org/10.1175/1520-0469(1980)037<1251:teocot>2.0.co;2)
- Hersey, S. P., Sorooshian, A., Murphy, S. M., Flagan, R. C., & Seinfeld, J. H. (2009). Aerosol hygroscopicity in the marine atmosphere: A closure study using high-time-resolution, multiple-RH DASH-SP and size-resolved C-ToF-AMS data. *Atmospheric Chemistry and Physics*, 9(7), 2543–2554.
- Hoffmann, F., Raasch, S., & Noh, Y. (2015). Entrainment of aerosols and their activation in a shallow cumulus cloud studied with a coupled LCM-LES approach. *Atmospheric Research*, 156, 43–57. <https://doi.org/10.1016/j.atmosres.2014.12.008>
- Houghton, H. G. (1955). On the chemical composition of fog and cloud water. *Journal Of Meteorology*, 12(4), 355–357. [https://doi.org/10.1175/1520-0469\(1955\)012<0355:otccof>2.0.co;2](https://doi.org/10.1175/1520-0469(1955)012<0355:otccof>2.0.co;2)
- Jiang, H., Feingold, G., Jonsson, H. H., Lu, M.-L., Chuang, P. Y., Flagan, R. C., & Seinfeld, J. H. (2008). Statistical comparison of properties of simulated and observed cumulus clouds in the vicinity of Houston during the Gulf of Mexico atmospheric composition and climate study (GOMACCS). *Journal of Geophysical Research-Atmospheres*, 113(d13). <https://doi.org/10.1029/2007jd009304>
- Johnson, B. T., Shine, K. P., & Forster, P. M. (2004). The semi-direct aerosol effect: Impact of absorbing aerosols on marine stratocumulus. *Quarterly Journal of The Royal Meteorological Society*, 130(599, b), 1407–1422. <https://doi.org/10.1256/qj.03.61>
- Jones, A., Haywood, J., & Boucher, O. (2009). Climate impacts of geoengineering marine stratocumulus clouds. *Journal of Geophysical Research-Atmospheres*, 114. <https://doi.org/10.1029/2008jd011450>
- Jones, A., & Slingo, A. (1996). Predicting cloud-droplet effective radius and indirect sulphate aerosol forcing using a general circulation model. *Quarterly Journal of The Royal Meteorological Society*, 122(535, a), 1573–1595.
- Katoshevski, D., Nenes, A., & Seinfeld, J. H. (1999). A study of processes that govern the maintenance of aerosols in the marine boundary layer. *Journal of Aerosol Science*, 30(4), 503–532. [https://doi.org/10.1016/S0021-8502\(98\)00740-X](https://doi.org/10.1016/S0021-8502(98)00740-X)
- Keene, W. C., Galloway, J. N., Likens, G. E., Deviney, F. A., Mikkelsen, K. N., Moody, J. L., & Maben, J. R. (2015). Atmospheric wet deposition in remote regions: Benchmarks for environmental change. *Journal of the Atmospheric Sciences*, 72(8), 2947–2978. <https://doi.org/10.1175/Jas-D-14-0378.1>
- Khairoutdinov, M., & Kogan, Y. (2000). A new cloud physics parameterization in a large-eddy simulation model of marine stratocumulus. *Monthly Weather Review*, 128(1), 229–243. [https://doi.org/10.1175/1520-0493\(2000\)128<0229:ancppi>2.0.co;2](https://doi.org/10.1175/1520-0493(2000)128<0229:ancppi>2.0.co;2)
- Kiehl, J. T., Schneider, T. L., Rasch, P. J., Barth, M. C., & Wong, J. (2000). Radiative forcing due to sulfate aerosols from simulations with the national center for atmospheric research community climate model, version 3. *Journal of Geophysical Research-Atmospheres*, 105(d1), 1441–1457. <https://doi.org/10.1029/1999jd900495>
- Koch, D., & Del Genio, A. D. (2010). Black carbon semi-direct effects on cloud cover: review and synthesis. *Atmospheric Chemistry and Physics*, 10(16), 7685–7696. <https://doi.org/10.5194/acp-10-7685-2010>
- Lance, S., Nenes, A., Mazzoleni, C., Dubey, M. K., Gates, H., Varutbangkul, V., et al. (2009). Cloud condensation nuclei activity, closure, and droplet growth kinetics of Houston aerosol during the Gulf of Mexico Atmospheric Composition and Climate Study (GOMACCS). *Journal of Geophysical Research-Atmospheres*, 114. <https://doi.org/10.1029/2008jd011699>
- Liu, Y. G., & Hallett, J. (1997). The '1/3' power law between effective radius and liquid-water content. *Quarterly Journal of The Royal Meteorological Society*, 123(542, b), 1789–1795. <https://doi.org/10.1002/qj.49712354220>
- Lohmann, U., & Feichter, J. (1997). Impact of sulfate aerosols on albedo and lifetime of clouds: A sensitivity study with the echam4 GCM. *Journal of Geophysical Research-Atmospheres*, 102(d12), 13685–13700. <https://doi.org/10.1029/97jd00631>
- Loye-pilot, M. D., & Morelli, J. (1988). Fluctuations of ionic composition of precipitations collected in Corsica related to changes in the origins of incoming aerosols. *Journal of Aerosol Science*, 19(5), 577–585. [https://doi.org/10.1016/0021-8502\(88\)90209-1](https://doi.org/10.1016/0021-8502(88)90209-1)
- Lu, M. L., Feingold, G., Jonsson, H. H., Chuang, P. Y., Gates, H., Flagan, R. C., & Seinfeld, J. H. (2008). Aerosol-cloud relationships in continental shallow cumulus. *Journal Of Geophysical Research-Atmospheres*, 113(d15). <https://doi.org/10.1029/2007jd008000>
- Lu, Z., Liu, X. H., Zhang, Z. B., Zhao, C., Meyer, K., Rajapakshe, C., et al. (2018). Biomass smoke from southern Africa can significantly enhance the brightness of stratocumulus over the southeastern Atlantic Ocean. *Proceedings of the National Academy of Sciences of the United States of America*, 115(12), 2924–2929. <https://doi.org/10.1073/pnas.1713703115>
- MacDonald, A. B., Dadashazar, H., Chuang, P. Y., Crosbie, E., Wang, H., Wang, Z., et al. (2018). Characteristic vertical profiles of cloud water composition in marine stratocumulus clouds and relationships with precipitation. *Journal of Geophysical Research: Atmospheres*, 123(7), 3704–3723. <https://doi.org/10.1002/2017jd027900>



- Mardi, A. H., Dadashazar, H., Macdonald, A. B., Braun, R. A., Crosbie, E., Xian, P., et al. (2018). Biomass burning plumes in the vicinity of the California coast: Airborne characterization of physicochemical properties, heating rates, and spatiotemporal features. *Journal of Geophysical Research: Atmospheres*, 123(23), 13560–13582. <https://doi.org/10.1029/2018jd029134>
- Martin, G. M., Johnson, D. W., & Spice, A. (1994). The measurement and parameterization of effective radius of droplets in warm stratocumulus clouds. *Journal of The Atmospheric Sciences*, 51(13), 1823–1842. [https://doi.org/10.1175/1520-0469\(1994\)051<1823:tma-poe>2.0.co;2](https://doi.org/10.1175/1520-0469(1994)051<1823:tma-poe>2.0.co;2)
- Maudlin, L. C., Wang, Z., Jonsson, H. H., & Sorooshian, A. (2015). Impact of wildfires on size-resolved aerosol composition at a coastal California site. *Atmospheric Environment*, 119, 59–68. <https://doi.org/10.1016/j.atmosenv.2015.08.039>
- Korolev, A. V., & Mazin, I. P. (1993). Zones of increased and decreased droplet concentration in stratiform clouds. *Journal of Applied Meteorology*, 32(4), 760–773. [https://doi.org/10.1175/1520-0450\(1993\)032<0760:zoiaadd>2.0.co;2](https://doi.org/10.1175/1520-0450(1993)032<0760:zoiaadd>2.0.co;2)
- McComiskey, A., Feingold, G., Frisch, A. S., Turner, D. D., Miller, M. A., Chiu, J. C., et al. (2009). An assessment of aerosol-cloud interactions in marine stratus clouds based on surface remote sensing. *Journal of Geophysical Research-Atmospheres*, 114. <https://doi.org/10.1029/2008jd011006>
- Meskhidze, N., Chameides, W. L., & Nenes, A. (2005). Dust and pollution: A recipe for enhanced ocean fertilization? *Journal of Geophysical Research-Atmospheres*, 110(D3). <https://doi.org/10.1029/2004jd005082>
- Modini, R. L., Frossard, A. A., Ahlm, L., Russell, L. M., Corrigan, C. E., Roberts, G. C., et al. (2015). Primary marine aerosol-cloud interactions off the coast of California. *Journal of Geophysical Research: Atmospheres*, 120, 4282–4303. <https://doi.org/10.1002/2014jd022963>
- Moritz, M. A., Parisien, M. A., Battlori, E., Krawchuk, M. A., Van Dorn, J., Ganz, D. J., & Hayhoe, K. (2012). Climate change and disruptions to global fire activity. *Ecosphere*, 3(6). <https://doi.org/10.1890/es11-00345.1>
- Nenes, A., & Seinfeld, J. H. (2003). Parameterization of cloud droplet formation in global climate models. *Journal of Geophysical Research-Atmospheres*, 108(d14). <https://doi.org/10.1029/2002jd002911>
- Ng, N. L., Canagaratna, M. R., Jimenez, J. L., Chhabra, P. S., Seinfeld, J. H., & Worsnop, D. R. (2011). Changes in organic aerosol composition with aging inferred from aerosol mass spectra. *Atmospheric Chemistry and Physics*, 11(13), 6465–6474.
- Novakov, T., Riveracarpio, C., Penner, J. E., & Rogers, C. F. (1994). The effect of anthropogenic sulfate aerosols on marine cloud droplet concentrations. *Tellus Series B-Chemical and Physical Meteorology*, 46(2), 132–141. <https://doi.org/10.1034/j.1600-0889.1994.t01-1-00005.x>
- O'Dowd, C. D., Aalto, P., Hameri, K., Kulmala, M., & Hoffmann, T. (2002). Aerosol formation - Atmospheric particles from organic vapours. *Nature*, 416(6880), 497–498. <https://doi.org/10.1038/416497a>
- O'Dowd, C. D., Lowe, J. A., Smith, M. H., & Kaye, A. D. (1999). The relative importance of non-sea-salt sulphate and sea-salt aerosol to the marine cloud condensation nuclei population: an improved multi-component aerosol-cloud droplet parametrization. *Quarterly Journal of The Royal Meteorological Society*, 125(556, b), 1295–1313. <https://doi.org/10.1256/smsqj.55609>
- Painemal, D., & Zuidema, P. (2011). Assessment of MODIS cloud effective radius and optical thickness retrievals over the southeast pacific with vocals-rex in situ measurements. *Journal of Geophysical Research-Atmospheres*, 116. <https://doi.org/10.1029/2011jd016155>
- Petrenchuk, O. P., & Drozdova, V. M. (1966). On chemical composition of cloud water. *Tellus*, 18(2–3), 280–. <https://doi.org/10.1111/j.2153-3490.1966.tb00238.x>
- Prabhakar, G., Ervens, B., Wang, Z., Maudlin, L. C., Coggon, M. M., Jonsson, H. H., et al. (2014). Sources of nitrate in stratocumulus cloud water: Airborne measurements during the 2011 e-peace and 2013 nice studies. *Atmospheric Environment*, 97(SI), 166–173. <https://doi.org/10.1016/j.atmosenv.2014.08.019>
- Raga, G. B., & Jonas, P. R. (1993). On the link between cloud-top radiative properties and sub-cloud aerosol concentrations. *Quarterly Journal of The Royal Meteorological Society*, 119(514), 1419–1425. <https://doi.org/10.1256/smsqj.51409>
- Rajapakse, C., Zhang, Z., Yorks, J. E., Yu, H., Tan, Q., Meyer, K., et al. (2017). Seasonally transported aerosol layers over southeast Atlantic are closer to underlying clouds than previously reported. *Geophysical Research Letters*, 44, 5818–5825. <https://doi.org/10.1002/2017GL073559>
- Reid, J. S., Hobbs, P. V., Ferek, R. J., Blake, D. R., Martins, J. V., Dunlap, M. R., & Liouss, C. (1998). Physical, chemical, and optical properties of regional hazes dominated by smoke in brazil. *Journal of Geophysical Research-Atmospheres*, 103(d24), 32059–32080. <https://doi.org/10.1029/98jd00458>
- Reid, J. S., Hobbs, P. V., Rangno, A. L., & Hegg, D. A. (1999). Relationships between cloud droplet effective radius, liquid water content, and droplet concentration for warm clouds in brazil embedded in biomass smoke. *Journal of Geophysical Research Atmospheres*, 104(d6), 6145–6153. <https://doi.org/10.1029/1998jd200119>
- Rhoades, C., Elder, K., & Greene, E. (2010). The influence of an extensive dust event on snow chemistry in the southern Rocky Mountains (vol 42, pg 102, 2010). *Arctic, Antarctic, And Alpine Research*, 42(4), 497. <https://doi.org/10.1657/1938-4246-42.4.497b>
- Rotstain, L. D. (1999). Indirect forcing by anthropogenic aerosols: A global climate model calculation of the effective-radius and cloud-lifetime effects. *Journal of Geophysical Research-Atmospheres*, 104(d8), 9369–9380. <https://doi.org/10.1029/1998jd900009>
- Russell, L. M., Sorooshian, A., Seinfeld, J. H., Albrecht, B. A., Nenes, A., Ahlm, L., et al. (2013). Eastern pacific emitted aerosol cloud experiment. *Bulletin of The American Meteorological Society*, 94(5), 709+. <https://doi.org/10.1175/bams-d-12-00015.1>
- Sanchez, K. J., Russell, L. M., Modini, R. L., Frossard, A. A., Ahlm, L., Corrigan, C. E., et al. (2016). Meteorological and aerosol effects on marine cloud microphysical properties. *Journal Of Geophysical Research-Atmospheres*, 121(8), 4142–4161. <https://doi.org/10.1002/2015JD024595>
- Schlosser, J. S., Braun, R. A., Bradley, T., Dadashazar, H., Macdonald, A. B., Aldhaif, A. A., et al. (2017). Analysis of aerosol composition data for western United States wildfires between 2005 and 2015: dust emissions, chloride depletion, and most enhanced aerosol constituents. *Journal of Geophysical Research: Atmospheres*, 122, 8951–8966. <https://doi.org/10.1002/2017jd026547>
- Schwikowski, M., Seibert, P., Baltensperger, U., & Gaggeler, H. W. (1995). A study of an outstanding Saharan dust event at the high-alpine site Jungfraujoch, Switzerland. *Atmospheric Environment*, 29(15), 1829–1842. [https://doi.org/10.1016/1352-2310\(95\)00060-c](https://doi.org/10.1016/1352-2310(95)00060-c)
- Seinfeld, J. H., & Pandis, S. N. (2016). *Atmospheric chemistry and physics*, (3rd ed.). New York: Wiley-Interscience.
- Shingler, T., Crosbie, E., Ortega, A., Shiraiwa, M., Zuend, A., Beyersdorf, A., et al. (2016). Airborne characterization of subsaturated aerosol hygroscopicity and dry refractive index from the surface to 6.5 km during the SEAC<sup>4</sup>RS campaign. *Journal Of Geophysical Research-Atmospheres*, 121(8), 4188–4210. <https://doi.org/10.1002/2015JD024498>
- Shingler, T., Dey, S., Sorooshian, A., Brechtel, F. J., Wang, Z., Metcalf, A., et al. (2012). Characterisation and airborne deployment of a new counterflow virtual impactor inlet. *Atmospheric Measurement Techniques*, 5(6), 1259–1269. <https://doi.org/10.5194/amt-5-1259-2012>
- Simpson, E., Connolly, P., & McFiggans, G. (2014). An investigation into the performance of four cloud droplet activation parameterizations. *Geoscientific Model Development*, 7(4), 1535–1542. <https://doi.org/10.5194/gmd-7-1535-2014>

- Slawinska, J., Grabowski, W. W., Pawlowska, H., & Morrison, H. (2012). Droplet activation and mixing in large-eddy simulation of a shallow cumulus field. *Journal of The Atmospheric Sciences*, 69(2), 444–462. <https://doi.org/10.1175/jas-d-11-054.1>
- Slingo, A. (1990). Sensitivity of the Earth's radiation budget to changes in low clouds. *Nature*, 343(6253), 49. <https://doi.org/10.1029/JD095iD10p16601>
- Sorooshian, A., Anderson, B., Bauer, S. E., Braun, R. A., Cairns, B., Crosbie, E., et al. (2019). Aerosol-cloud-meteorology interaction airborne field investigations: Using lessons learned from the US West Coast in the design of ACTIVATE off the US East Coast. *Bulletin of The American Meteorological Society*, 2019. <https://doi.org/10.1175/BAMS-D-18-0100.1>
- Sorooshian, A., Crosbie, E., Maudlin, L. C., Youn, J.-S., Wang, Z., Shingler, T., et al. (2015). Surface and airborne measurements of organosulfur and methanesulfonate over the western United States and coastal areas. *Journal of Geophysical Research: Atmospheres*, 120, 8535–8548. <https://doi.org/10.1002/2015jd023822>
- Sorooshian, A., Macdonald, A. B., Dadashazar, H., Bates, K. H., Coggon, M. M., Craven, J. S., et al. (2018). A multi-year data set on aerosol-cloud-precipitation-meteorology interactions for marine stratocumulus clouds. *Scientific Data*, 5. <https://doi.org/10.1038/sdata.2018.26>
- Sorooshian, A., Shingler, T., Harpold, A., Feagles, C. W., Meixner, T., & Brooks, P. D. (2013). Aerosol and precipitation chemistry in the southwestern United States: Spatiotemporal trends and interrelationships. *Atmospheric Chemistry and Physics*, 13(15), 7361–7379. <https://doi.org/10.5194/acp-13-7361-2013>
- Sorooshian, A., Wang, Z., Coggon, M. M., Jonsson, H. H., & Ervens, B. (2013). Observations of sharp oxalate reductions in stratocumulus clouds at variable altitudes: Organic acid and metal measurements during the 2011 E-PEACE Campaign. *Environmental Science & Technology*, 47(14), 7747–7756. <https://doi.org/10.1021/es4012383>
- Stephens, G. L., & Greenwald, T. J. (1991). The Earth's radiation budget and its relation to atmospheric hydrology: 2. Observations of cloud effects. *Journal of Geophysical Research-Atmospheres*, 96(D8), 15325–15340. <https://doi.org/10.1029/91JD00972>
- Swap, R. J., Annegarn, H. J., & Otter, L. (2002). Southern African regional science initiative (safari 2000): summary of science plan. *South African Journal of Science*, 98(3–4), 119–124.
- Terai, C. R., Wood, R., Leon, D. C., & Zuidema, P. (2012). Does precipitation susceptibility vary with increasing cloud thickness in marine stratocumulus? *Atmospheric Chemistry and Physics*, 12(10), 4567–4583. <https://doi.org/10.5194/acp-12-4567-2012>
- Twohy, C. H., Petters, M. D., Snider, J. R., Stevens, B., Tahnk, W., Wetzell, M., et al. (2005). Evaluation of the aerosol indirect effect in marine stratocumulus clouds: droplet number, size, liquid water path, and radiative impact. *Journal of Geophysical Research-Atmospheres*, 110(d8). <https://doi.org/10.1029/2004jd005116>
- Wang, H., Easter, R. C., Rasch, P. J., Wang, M., Liu, X., Ghan, S. J., et al. (2013). Sensitivity of remote aerosol distributions to representation of cloud-aerosol interactions in a global climate model. *Geoscientific Model Development*, 6(3), 765–782. <https://doi.org/10.5194/gmd-6-765-2013>
- Wang, Z., Ramirez, M. M., Dadashazar, H., Macdonald, A. B., Crosbie, E., Bates, K. H., et al. (2016). Contrasting cloud composition between coupled and decoupled marine boundary layer clouds. *Journal of Geophysical Research: Atmospheres*, 121, 11679–11691. <https://doi.org/10.1002/2016jd025695>
- Wang, Z., Sorooshian, A., Prabhakar, G., Coggon, M. M., & Jonsson, H. H. (2014). Impact of emissions from shipping, land, and the ocean on stratocumulus cloud water elemental composition during the 2011 E-PEACE field campaign. *Atmospheric Environment*, 89, 570–580. <https://doi.org/10.1016/j.atmosenv.2014.01.020>
- Warren, G., Hahn, J., London, J., Chervin, M., & Jenne, L. (1986). Global distribution of total cloud cover and cloud type amounts over land. <https://doi.org/10.5065/D6GH9FXB>
- Wilcox, E. M. (2012). Direct and semi-direct radiative forcing of smoke aerosols over clouds. *Atmospheric Chemistry and Physics*, 12(1), 139–149. <https://doi.org/10.5194/acp-12-139-2012>
- Williams, M. W., & Melack, J. M. (1991). Solute chemistry of snowmelt and runoff in an alpine basin, Sierra-Nevada. *Water Resources Research*, 27(7), 1575–1588. <https://doi.org/10.1029/90wr02774>
- Wonaschuetz, A., Coggon, M., Sorooshian, A., Modini, R., Frossard, A. A., Ahlm, L., et al. (2013). Hygroscopic properties of smoke-generated organic aerosol particles emitted in the marine atmosphere. *Atmospheric Chemistry and Physics*, 13(19), 9819–9835. <https://doi.org/10.5194/acp-13-9819-2013>
- Wood, R. (2012). Stratocumulus clouds. *Monthly Weather Review*, 140(8), 2373–2423. <https://doi.org/10.1175/mwr-d-11-00121.1>
- Wood, R., Leon, D., Lebsock, M., Snider, J., & Clarke, A. D. (2012). Precipitation driving of droplet concentration variability in marine low clouds. *Journal of Geophysical Research-Atmospheres*, 117. <https://doi.org/10.1029/2012jd018305>
- Zuidema, P., Redemann, J., Haywood, J., Wood, R., Piketh, S., Hipondoka, M., & Formenti, P. (2016). Smoke and Clouds above the Southeast Atlantic Upcoming Field Campaigns Probe Absorbing Aerosol's Impact on Climate. *Bulletin of the American Meteorological Society*, 97(7), 1131–1135.